MedChemComm

RESEARCH ARTICLE

View Article Online
View Journal | View Issue

Cite this: *Med. Chem. Commun.*, 2019, **10**, 991

Scaffold hybridization strategy towards potent hydroxamate-based inhibitors of *Flaviviridae* viruses and *Trypanosoma* species†

Erofili Giannakopoulou,[a] Vasiliki Pardali,[a] Efseveia Frakolaki,[b] Vasileios Siozos,[b] Vassilios Myrianthopoulos,[a] Emmanuel Mikros,[a] Martin C. Taylor,[c] John M. Kelly,‡[c] Niki Vassilaki§[b] and Grigoris Zoidis ¶*[a]

Infections with *Flaviviridae* viruses, such as hepatitis C virus (HCV) and dengue virus (DENV) pose global health threats. Infected individuals are at risk of developing chronic liver failure or haemorrhagic fever respectively, often with a fatal outcome if left untreated. Diseases caused by tropical parasites of the *Trypanosoma* species, *T. brucei* and *T. cruzi*, constitute significant socioeconomic burden in sub-Saharan Africa and continental Latin America, yet drug development is under-funded. Anti-HCV chemotherapy is associated with severe side effects and high cost, while dengue has no clinically approved therapy and antiparasitic drugs are outdated and difficult to administer. Moreover, drug resistance is an emerging concern. Consequently, the need for new revolutionary chemotherapies is urgent. By utilizing a molecular framework combination approach, we combined two distinct chemical entities with proven antiviral and trypanocidal activity into a novel hybrid scaffold attached by an acetohydroxamic acid group (CH_2-CONHOH), aiming at derivatives with dual activity. The novel spiro-carbocyclic substituted hydantoin analogues were rationally designed, synthesized and evaluated for their potency against three HCV genotypes (1b, 3a, 4a), DENV and two *Trypanosoma* species (*T. brucei*, *T. cruzi*). They exhibited significant EC_{50} values and remarkable selectivity indices. Several modifications were undertaken to further explore the structure activity relationships (SARs) and confirm the pivotal role of the acetohydroxamic acid metal binding group.

Received 2nd April 2019,
Accepted 15th May 2019

DOI: 10.1039/c9md00200f

rsc.li/medchemcomm

Introduction

Hepatitis C virus (HCV) is a global health burden with ~71 million people estimated to be infected.[1] It is a main cause of chronic liver disease and can lead to liver cirrhosis and hepatocellular carcinoma. HCV is a member of the *Flaviviridae* family and belongs to the *Hepacivirus* genus.[2] The viral genome is a 9600 nucleotide-long single-stranded RNA of positive polarity and encodes a single polyprotein precursor, which is processed into structural proteins (core, E1 and E2), p7 required for assembly and release of virus particles and six non-structural (NS) proteins (NS2, NS3, NS4A, NS4B, NS5A and NS5B).[3,4] The NS proteins form a membrane-associated replicase complex (RC) in association with host cell factors. HCV is classified into 8 major genotypes and at least 86 sub/genotypes (GTs),[5] with genotype 1 being the most predominant type worldwide.[6]

Until recently, the standard of care for HCV was ribavirin and pegylated–interferon alpha (PEG–IFN), which had severe side effects and low sustained virologic response (SVR) rates.[7] Since 2011, direct-acting antivirals (DAAs) targeting the viral NS3/4A protease, the NS5B RNA-dependent RNA polymerase (RdRp) and the NS5A phosphoprotein were introduced (Fig. 1)[8–11] and allowed the implementation of interferon-free treatment schedules,[12,13] which are able to attain SVR in more than 90% of patients.[14] DAAs efficacy differs between genotypes, with genotype 3 elimination rate being lower than the others.[15,16]

However, there is a risk for the development of antiviral drug resistance, depending on the regimen and the genotype.[17] Moreover, available DAAs are costly, limiting their widespread clinical use, and, as a result, therapy remains low on a global scale.[18] Thus, there is still a need for novel effective drugs of lower cost.

[a] *School of Health Sciences, Faculty of Pharmacy, Department of Pharmaceutical Chemistry, National and Kapodistrian University of Athens, Panepistimiopolis-Zografou, GR-15771 Athens, Greece. E-mail: zoidis@pharm.uoa.gr*
[b] *Molecular Virology Laboratory, Hellenic Pasteur Institute, Vas. Sofias Avenue, GR-11521, Athens, Greece*
[c] *Department of Pathogen Molecular Biology, London School of Hygiene and Tropical Medicine, Keppel Street, London WC1E 7HT, UK*

† Electronic supplementary information (ESI) available. See DOI: 10.1039/c9md00200f

‡ Principal investigator of the study on *Trypanosoma* species.
§ Principal investigator of the study on *Flaviviridae* viruses.
¶ Principal investigator of the design and synthesis of the compounds.

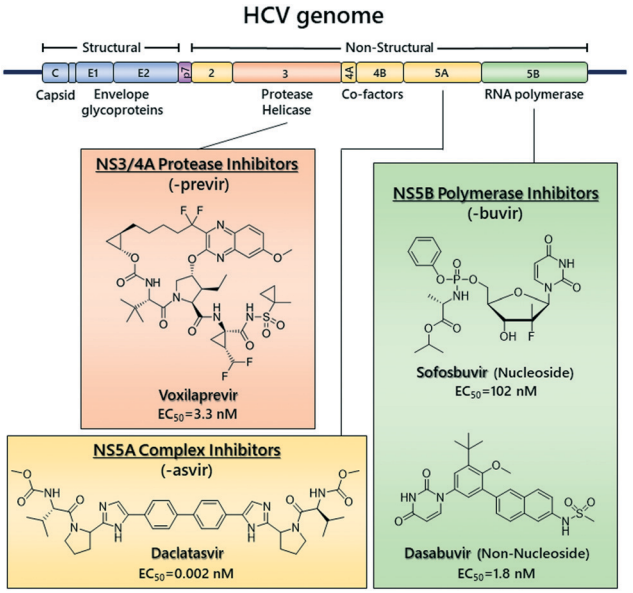

Fig. 1 Representative chemical structures of clinically approved DAAs and their respective EC_{50}s against HCV genotype 1b.

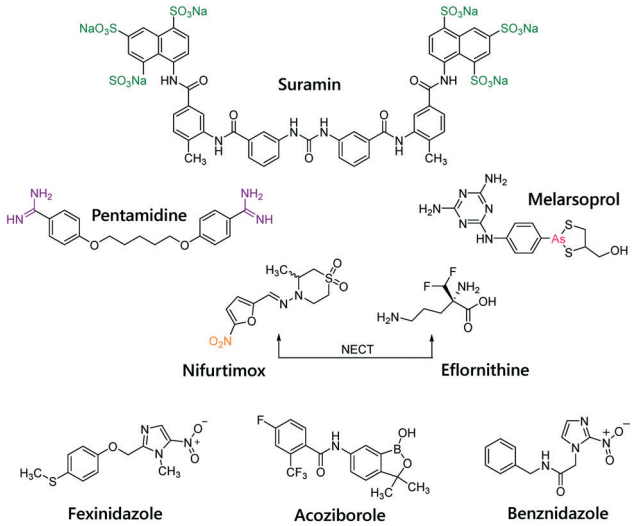

Fig. 2 Currently available marketed drugs for treatment of HAT and Chagas disease. Highlighted regions are reported to play a major role in the mechanism of action. Chemical structures of potential drug candidates fexinidazole and acoziborole.

The mosquito-borne dengue virus (DENV) is another member of the *Flaviviridae* family, belonging to the *Flavivirus* genus. It causes widely distributed and endemic, visceral and central nervous system diseases.[19] Symptoms of infection range from mild (dengue fever) to the more severe dengue hemorrhagic fever (DHF) and dengue shock syndrome (DSS).[20] The recently approved dengue vaccine has only limited overall efficacy[21] and there is no approved antiviral therapy.[22] DENV genome consists of a positive single-stranded RNA of ~11 kb in length, encoding for the viral polyprotein, which is processed into structural proteins (C, prM, E) and non-structural proteins (NS1, NS2A, NS2B, NS3, NS4A, NS4B, NS5).[23,24]

Bivalent metal ions are important for the stability and activity of various HCV and DENV proteins, including NS3 helicase/protease, RdRp polymerase and HCV NS5A protein.[25–30]

Human African trypanosomiasis (HAT), also known as sleeping sickness, is a vector-borne parasitic disease with 65 million people being vulnerable to infection.[31] HAT occurs in 36 countries of sub-Saharan Africa and it is caused by infection with protozoan parasites belonging to the *Trypanosoma brucei* sp. *T. b. gambiense* is the causative agent of a chronic form of the disease (*gambiense* HAT, gHAT). It is prevalent in central and western Africa, and can take years or decades to produce a fatal outcome. *T. b. rhodesiense* is responsible for an acute form disease, causing death within weeks or months of infection. *Rhodesiense* HAT (rHAT) is found in eastern and southern Africa.[32,33] Clinical progression of both forms of HAT is divided in two stages. The early hemolymphatic stage and the late meningoencephalitic stage when the parasites enter the central nervous system causing neurological damage and sleep disturbances.[34]

Treatment approaches of HAT consist of five drugs: pentamidine, suramin, melarsoprol, eflornithine, and nifurtimox–eflornithine combination therapy (NECT) (Fig. 2). Nevertheless, their increasing levels of resistance, their limited efficacy, toxicity and adverse side effects, make HAT treatment a daunting challenge.[35] Fexinidazole and acoziborole (Fig. 2) are two potential drug candidates, currently being in advanced clinical trials.[36,37]

American trypanosomiasis, or Chagas disease, is a potentially life-threatening infection caused by the protozoan parasite *Trypanosoma cruzi*. It is endemic in continental Latin America, with a devastating effect upon 6–7 million people,[38] and it is characterized by two distinct clinical phases: an acute mostly asymptomatic phase, and a chronic phase characterized mainly by cardiac disorders.[39] The two drugs available, nifurtimox and benznidazole (Fig. 2), are only partially effective and toxic side effects limit their use.[40]

Unfortunately, there is no efficient disease management for both parasitic infections and the World Health Organization has listed them among the neglected tropical diseases (NTDs). Therefore, in absence of vaccines, development of novel effective therapeutics is an imperative for their treatment and control.[33]

Several groups of trypanosomatid metalloenzymes have been identified as playing an important role in the metabolism and viability of parasites. Amongst the most widely explored are histone deacetylases (HDACs), trypanosome alternative oxidase (TAO) and carbonic anhydrase (CA).[41–48]

Metalloenzymes' inhibition appears attractive as a chemotherapeutic approach against viruses and parasites.[47–53] It has been proved that the vast majority of metalloenzyme inhibitors are chelating agents employing metal binding groups to coordinate the active site metal ion.[54,55] As a continuation of our research on metal chelating agents,[56,57] we were interested in developing novel combined scaffolds demonstrating both antiviral and antiparasitic properties.

In this study, we report the rational design and synthesis of novel spiro-hydantoin analogues, attached by the aceto-hydroxamic acid moiety ($CH_2CONHOH$) as the potential metal binding functional group (Fig. 3). Several bicyclic fused rings were used as spiro-substituents on the basic 2,4-diketoimidazolidine scaffold, while methyl- and benzyl-groups were incorporated at the amide nitrogen atom of hydantoin, to enhance binding affinity and improve drug-likeness of the compounds. The novel analogues were assessed as antiviral and trypanocidal agents and exhibited remarkable inhibitory activity with respect to their parent compounds **I** and **II**. More specifically, they were evaluated for their effect on RNA replication and cell viability on different HCV genotypes (1b, 3a, 4a) and DENV. Their antiparasitic activity was assessed based on their ability to inhibit proliferation of cultured bloodstream form *T. brucei* and *T. cruzi* epimastigotes *in vitro*.

Results and discussion

Rational design – theoretical calculations

Previous studies by our group have resulted in compounds carrying metal chelating moieties that demonstrated a highly promising inhibition capacity against either pathogenic viruses, including influenza and HCV,[56] or parasites of the *Trypanosoma* genus.[57,58] The two above-mentioned series of analogues, although structurally diverse, were based on rational incorporation of metal chelating moieties on scaffolds with pronounced drug-likeness, such as the combination of flutimide with the indole system (**I**) or incorporation of the acetohydroxamic acid moiety on a 2,6-diketopiperazine (2,6-DKP) scaffold (**II**) (Fig. 3). In the present study, a conceptual approach to further exploit the bioactivity of molecules with potential metal chelating efficacy toward designing effectors with inhibitory activity against both disease-related viruses and *Trypanosoma* parasites is reported. The design was based on combination of the exocyclic acetohydroxamic acid pharmacophore, bearing well proven trypanocidal activity, with a lipophilic tail based on a bicyclic system-substituted hydantoin that could effectively mimic the antiviral flutimide scaffold yet with increased steric bulk, thus affording a novel synthetically tractable heterocyclic scaffold as presented in detail in Fig. 3.

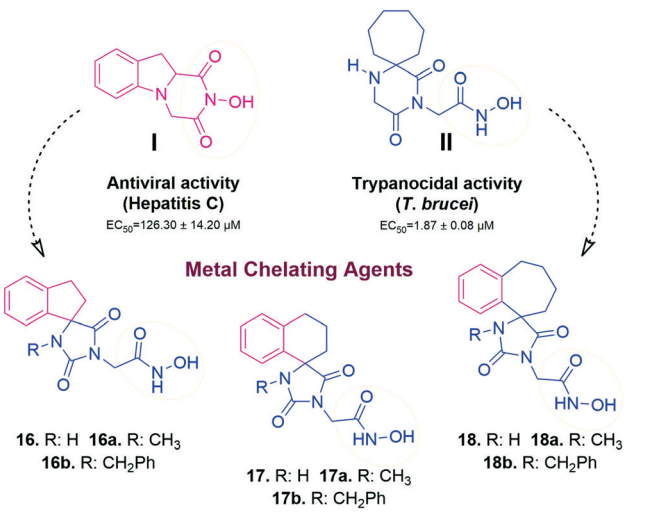

Fig. 3 Indole–flutimide analogue (I) with antiviral activity, cycloheptane spiro-substituted 2,6-DKP analogue (II) with trypanocidal activity and novel synthesized analogues reported in this study. Metal binding groups are indicated in plum elliptical shape.

To counterbalance possible issues of water solubility arising from the tricyclic system of the antiviral lead **I**, we selected to enhance the sp^3 character of the novel scaffold by introducing a spiro connection between the acetohydroxamic group-carrying hydantoin and the indane system. In this case, resembling the spiro trypanocidal lead **II** would contribute toward avoiding possible Lipinski's rule-of-five violations. Hence, the indole nitrogen atom was converted to a carbon, giving rise to a hydrophobic indane (compound **16**). Moreover, with the aim of evaluating the contribution of the critical parameter of lipophilicity on biological activity, extensions of the indane system to tetralin or benzocycloheptane were considered (compounds **17** and **18**), while the addition of alkyl substituents such as methyl- or benzyl-groups on N3 of hydantoin was also explored (compounds **16a**, **17a**, **18a** and **16b**, **17b**, **18b** respectively). To confirm the importance of the exocyclic acetohydroxamic acid moiety on antiviral and trypanocidal activity, the derivative **4**, lacking metal chelating ability, was evaluated as a negative control (Tables 1 and 2). The derivative **16** carrying the smallest steric bulk, *i.e.* an indane system with no substitution on N3, was selected for probing the validity of our approach.

Compound **16** was synthesized and subsequently tested against HCV (replicon 1b) and bloodstream form *T. brucei in vitro*, exhibiting significant inhibitory activity against both targets. More specifically, the EC_{50} value for HCV was in the low micromolar range (EC_{50} **16** = 2.92 μM, Table 1) and for *T. brucei* was in the nanomolar range (EC_{50} **16** = 0.44 μM, Table 2), identifying this particular acetohydroxamic acid derivative as a promising and original lead compound. All the aforementioned designed analogues were also synthesized and tested against two different genotypes of HCV (1b and 4a) and against two *Trypanosoma* species. Analogues **16**, **17** and **18** were also tested against HCV genotype 3a and DENV. The resulting EC_{50} and cytotoxicity values are presented in Tables 1 and 2.

Chemistry

As depicted in Scheme 1, the commercially available ketones **1–3** (Scheme 1A) were subjected to Bucherer–Bergs reaction with ammonium carbonate and potassium/sodium cyanide in $EtOH/H_2O$. Treatment of the resulting hydantoins **4–6** with potassium bis(trimethylsilyl)amide in dry THF afforded the corresponding potassium imidate salts. The latter intermediates were converted to the respective benzyl esters **7–9** upon S_N2 reaction with benzyl

Table 1 *In vitro* inhibitory activity of compounds **16–18**, **16a–18a**, **16b–18b** and hydantoin analogue **4** tested against HCV (genotypes 1b, 3a, 4a) and DENV (serotype 2). Cytotoxicity against Huh5-2, HCV replicon cells and selectivity indices

			HCV-1b		HCV-3a		HCV-4a		DENV-2		
Structure	Cmpd	R	EC_{50}[a] (μM)	SI[b]	EC_{50}[a] (μM)	SI[b]	EC_{50}[a] (μM)	SI[b]	EC_{50}[a] (μM)	SI[b]	CC_{50}[c] (μM)
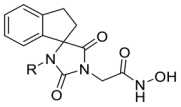	**16**	H	**2.92 ± 0.01**	>68	**2.97 ± 0.21**	>67	**0.58 ± 0.04**	>345	**96.34 ± 1.00**	>2	>200
	16a	CH_3	**1.41 ± 0.01**	19	—	—	**0.21 ± 0.02**	128	—	—	26.91 ± 0.67
	16b	CH_2Ph	**0.22 ± 0.01**	34	—	—	**0.14 ± 0.01**	54	—	—	7.53 ± 1.29
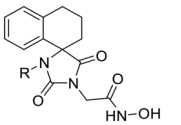	**17**	H	**1.41 ± 0.35**	>142	**2.37 ± 0.17**	>84	**0.38 ± 0.04**	>526	**61.49 ± 3.86**	>3	>200
	17a	CH_3	**1.45 ± 0.07**	99	—	—	**0.21 ± 0.01**	682	—	—	143.2 ± 0.37
	17b	CH_2Ph	**0.32 ± 0.01**	28	—	—	**0.07 ± 0.02**	127	—	—	8.90 ± 0.77
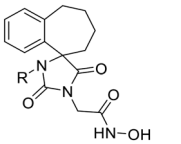	**18**	H	**0.25 ± 0.02**	794	**0.08 ± 0.01**	2480	**0.10 ± 0.00**	1984	**16.29 ± 2.17**	12	198.4 ± 2.24
	18a	CH_3	**1.18 ± 0.07**	95	—	—	**0.11 ± 0.01**	1015	—	—	111.6 ± 12.43
	18b	CH_2Ph	**1.00 ± 0.05**	5	—	—	**0.12 ± 0.01**	45	—	—	5.45 ± 0.27
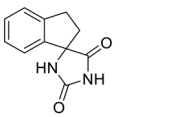	**4**	H	**>10**	—	—	—	—	—	—	—	>10
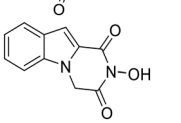	**I**	—	**126.30 ± 14.20**	>1.6	—	—	—	—	—	—	>200

[a] EC_{50} (median effective concentration) values represent the mean ± SD of three independent experiments, each carried out in triplicate. Calculated against HCV genotype 1b (Huh5-2, HCV 1b replicon cells), genotype 3a (Huh7.5-3a, HCV 3a replicon cells), genotype 4a (Huh7.5-4a, HCV 4a replicon cells). [b] Selectivity index: CC_{50}/EC_{50}. [c] CC_{50} (median cytotoxic concentration against Huh5-2, HCV replicon cells) values represent the mean ± SD of three independent experiments, each carried out in triplicate.

bromoacetate in dry DMF, as described in our previously published protocols.[59,60] Catalytic hydrogenolysis (Pd/C 10%) of the aforementioned benzyl esters led to the carboxylic acids **10–12**, which were further converted to the corresponding *O*-benzyl hydroxamates **13–15** upon coupling with *O*-benzylhydroxylamine·HCl in the presence of CDI or EDCI·HCl, HOBt. Finally, removal of the protective group was accomplished with hydrogenolysis, yielding almost quantitatively the target acetohydroxamic acids **16–18**.

For the synthesis of the *N*-alkylated analogues, the precursors benzyl esters **7–9** were reacted with NaH and the corresponding alkyl halide in dry DMF. Surprisingly, in the case of *N*-methylation procedure, transesterification products (methyl esters) were also isolated (Scheme 1C), along with the expected *N*-methylated benzyl esters.[59] Employment of the previously described methodology, catalytic hydrogenolysis of the benzyl esters **7a–9a** and **7b–9b**, followed by amidation and deprotection of the amides **13a–15a** and **13b–15b**, afforded the desired *N*-alkylated acetohydroxamic acids **16a–18a** and **16b–18b**.

Biology

Antiviral assays

Screening of compounds using an HCV genotype 1b replicon system. The effects of analogues **16–18**, **16a–18a**, **16b–18b** and **4** on HCV RNA replication and cell viability were determined in the stable cell line Huh5-2 containing an HCV genotype 1b (strain Con1) replicon encoding the firefly luciferase gene.[61] In this cell system, the level of expressed luciferase directly correlates with the level of HCV RNA replication. Using serial dilutions of the compounds, the half maximal effective concentration (EC_{50}) and the median cytotoxic concentration (CC_{50}) were obtained, by measuring HCV replication-driven luciferase activity and intracellular ATP levels, respectively (Table 1, Fig. 4A). Dose–response curve analysis is presented for the most potent analogue **18** (Fig. 4B). Selectivity indices (SI) = CC_{50}/EC_{50} were calculated for all analogues synthesized.

As shown in Table 1, acetohydroxamic acid analogues were potent against HCV-1b replication, with EC_{50} values ranging from 0.22 to 2.92 μM. Compounds **16b**, **17b** and **18** exhibited the highest inhibitory activity, with EC_{50}s in the submicromolar range (0.22 μM, 0.32 μM and 0.25 μM, respectively). We observed that the replacement of indane ring of **16** with the bulkier tetralin (**17**) and benzocycloheptane (**18**) rings progressively increased the activity of the compounds. It is noteworthy that the activity of **18** (EC_{50} = 0.25 μM) was 12-fold better than lead compound **16** (EC_{50} = 2.92 μM). A marked improvement was also observed on the EC_{50} value of **16** (43-fold lower), compared to the structurally related fused indole–flutimide analogue **I** (EC_{50} = 126.3 μM),[56] validating the idea of incorporating a spiro connection between hydantoin and the indane ring. Introduction of a methyl

Table 2 Activity of acetohydroxamic acid analogues **16**–**18**, **16a**–**18a**, **16b**–**18b** and hydantoin analogue **4** tested against cultured bloodstream form *T. brucei* (pH 7.4) and *T. cruzi* epimastigotes. Cytotoxicity against cultured rat skeletal myoblast L6 cells, selectivity indices, log *D* and pK_a values

			T. brucei			*T. cruzi*					
Structure	Cmpd	R	EC_{50}[a] (μM)	EC_{90}[a] (μM)	SI[b]	EC_{50}[a] (μM)	EC_{90}[a] (μM)	SI[b]	L6 cells CC_{50}[c] (μM)	log *D*[d] (pH 7.4)	pK_a[e]
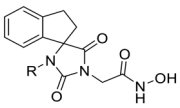	**16**	H	0.44 ± 0.08	0.80 ± 0.02	609	>30	>30	—	268 ± 9	−0.24	9.1
	16a	CH_3	1.22 ± 0.39	1.93 ± 0.45	451	>30	—	—	550 ± 24	−0.01	9.0
	16b	CH_2Ph	0.101 ± 0.003	0.192 ± 0.003	62	1.70 ± 0.06	3.01 ± 0.36	4	6.27 ± 0.60	1.71	9.5
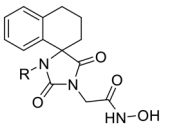	**17**	H	0.71 ± 0.12	1.27 ± 0.02	590	>30	>30	—	419 ± 55	0.21	9.3
	17a	CH_3	1.91 ± 0.23	4.69 ± 0.10	15	27.6 ± 5.3	42.1 ± 2.4	1	28.2 ± 1.0	0.43	9.0
	17b	CH_2Ph	0.050 ± 0.003	0.077 ± 0.021	63	0.96 ± 0.03	1.71 ± 0.07	3	3.17 ± 0.48	2.16	9.2
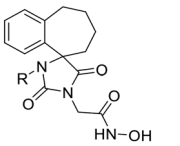	**18**	H	0.40 ± 0.04	0.52 ± 0.05	313	>30	—	—	125 ± 12	0.65	9.3
	18a	CH_3	0.23 ± 0.01	0.30 ± 0.01	71	10.6 ± 0.6	15.3 ± 0.2	2	16.4 ± 1.1	0.88	9.2
	18b	CH_2Ph	0.013 ± 0.002	0.018 ± 0.001	604	0.495 ± 0.058	0.94 ± 0.033	16	7.85 ± 0.33	2.60	9.4
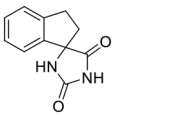	**4**	H	>50	—	—	>500	—	—	>500	0.89	n.a.
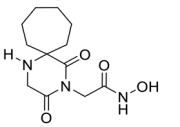	**II**	—	1.87 ± 0.08	2.53 ± 0.29	—	—	—	—	—	—	—

[a] Concentrations required to inhibit growth of *T. brucei* and *T. cruzi* by 50% and 90%, respectively. EC_{50} and EC_{90} data are the mean of triplicate experiments ± SEM. [b] Selectivity indices were calculated as the ratio of the CC_{50} for L6 cells to EC_{50} for *T. brucei* or *T. cruzi* respectively. [c] Cytotoxicity was determined by establishing the concentration required to inhibit growth of cultured L6 cells by 50% (CC_{50}). Data are the mean of triplicate experiments ± SEM. [d] log *D* at pH 7.4 determined using Marvin.[62] [e] pK_a values for the oxime proton determined from MM preoptimized geometries at the DFT(b3lyp) level with the cc-pVTZ(+) basis set using the Jaguar pK_a module of Maestro.[63–66]

substituent on the amide nitrogen atom of the 2,4-diketoimidazolidine scaffold of **16** led to a 2-fold increase in the activity (EC_{50} **16a** = 1.41 μM). However, this methylation had almost no effect in the potency of **17** (EC_{50} **17** = 1.41 μM; EC_{50} **17a** = 1.45 μM) and resulted in lower inhibitory potency for the *N*-methylated analogue **18a** (EC_{50} **18a** = 1.18 μM). The addition of the bulky lipophilic benzyl substituent to the same nitrogen atom of the hydantoin scaffold led to lower EC_{50} values for the resulting analogues **16b** (EC_{50} = 0.22 μM) and **17b** (EC_{50} = 0.32 μM), as compared to the addition of the methyl substituent. On the other hand, the benzyl group decreased the activity of compound **18b** 4-fold with respect to the corresponding NH-analogue **18**. In the case of the hydantoin **4**, the lack of activity underlines the importance of the acetohydroxamic acid metal binding group for the antiviral potency of the compounds.

Concerning the cytotoxicity evaluation (Table 1), all the non-substituted analogues **16**, **17** and **18** exhibited high CC_{50} values (≥200 μM), which resulted in remarkable selectivity indices. The most promising analogue appears to be compound **18**, with SI value of 794. It is of great interest that the incorporation of an alkyl substituent onto the amide nitrogen atom progressively increased the cytotoxicity of the compounds, in agreement with the higher lipophilicity determined by calculated log *D* values (Table 2); the bulkier the lipophilic substituent, the lower the CC_{50} value.

Activity of the compounds against other HCV genotypes. As the compounds exhibited significant potency against HCV genotype 1b, they were selected for further testing against other HCV genotypes. Specifically, we determined viral replication-derived luciferase activity in Huh7.5-3a stable cell line for compounds **16**, **17** and **18** and in Huh7.5-4a stable cell line for compounds **16**–**18**, **16a**–**18a** and **16b**–**18b**, containing subgenomic replicons of HCV genotype 3a (isolate S52) and 4a (isolate ED43), respectively.

Similar to genotype 1b, the activity of **16**, **17** and **18** against HCV genotype 3a ranged from low micromolar to nanomolar, and the increase in ring size conferred higher potency. Specifically, EC_{50} values were below 2.97 μM, with the most promising analogue being compound **18** (EC_{50} **18** = 0.08 μM; SI **18** = 2480), whose activity was 3-fold higher compared to the one exhibited in HCV-1b.

Biological evaluation of the hydroxamic acid derivatives on HCV-4a indicated enhanced activity as compared to genotypes 1b and 3a. All the novel synthesized analogues inhibited HCV-4a replication at submicromolar concentrations, ranging from 0.07 μM for **17b** to 0.58 μM for the indane substituted analogue **16**. Tetralin substitution

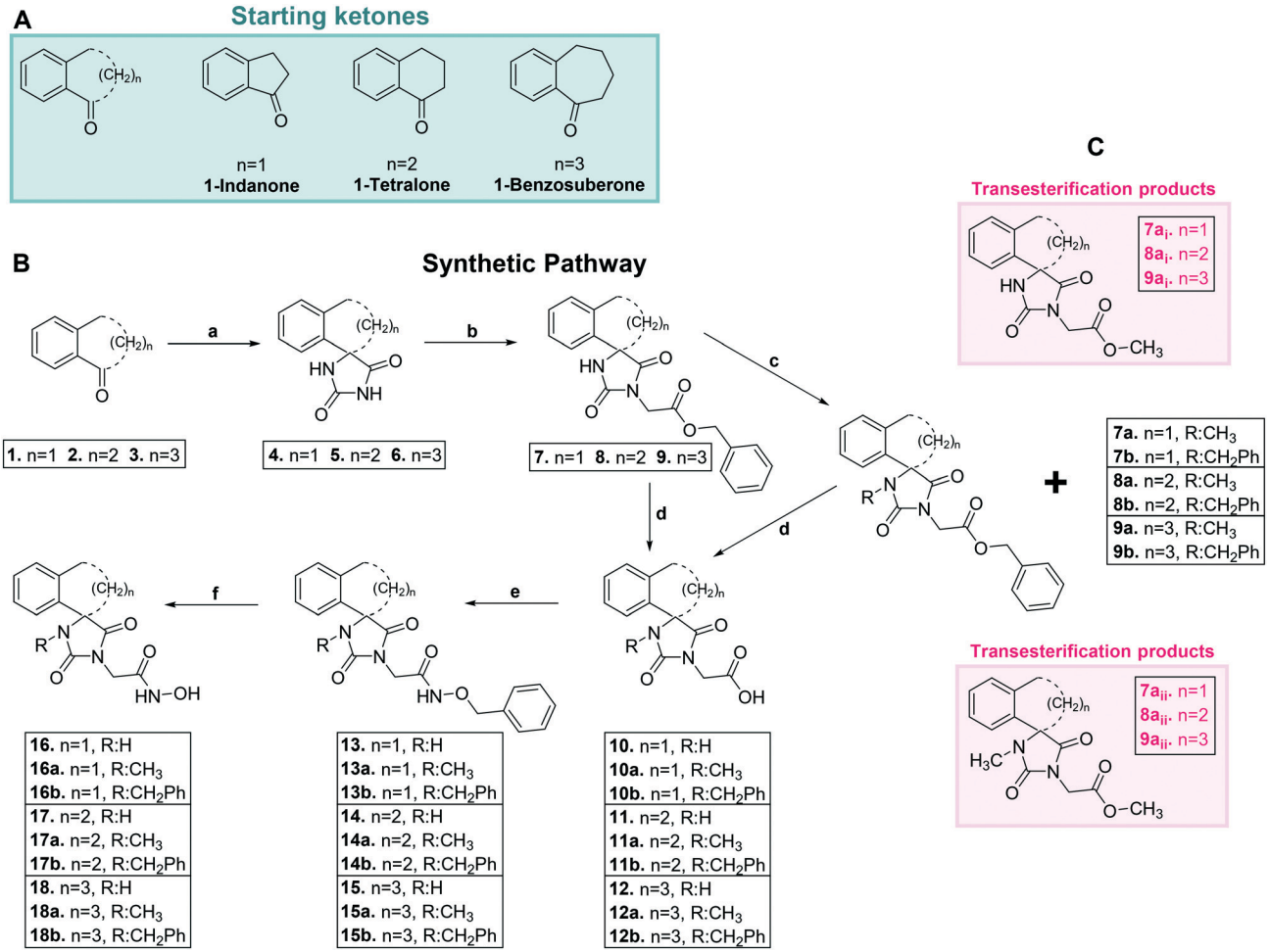

Scheme 1 A) Starting ketones B) synthesis of the target acetohydroxamic acid analogues **16**–**18**, **16a**–**18a** and **16b**–**18b**. Reagents and conditions: (a) method A: NaCN (2.27 eq.), $(NH_4)_2CO_3$ (6 eq.), EtOH/H_2O (1.1 : 1), reflux, 8 h–11 days; | method B: KCN (1.3 eq.), $(NH_4)_2CO_3$ (5 eq.), EtOH/H_2O (1 : 3), MW (100 W), 120 °C, 25 min–1 h; (b) (i) $[(CH_3)_3Si]_2NK$ (1.02 eq.), dry THF (0–5 °C) and then r.t., 20 min–1 h, argon; (ii) $BrCH_2COOCH_2Ph$ (1.05 eq.), dry DMF, 35–38 °C, 48 h, argon; (c) (i) NaH (1.2 eq.), dry DMF, (0–5 °C) and then r.t., 15 min, argon; (ii) $PhCH_2Br$ (1.2 eq.), 60 °C, 7 days, argon; (d) H_2, Pd/C 10%, EtOH/AcOEt 3 : 1, 50–55 psi, 40–45 °C, 3 h; (e) method A: EDCI·HCl (1.2 eq.), HOBt (1.2 eq.), $PhCH_2ONH_2$·HCl (1.2 eq.), TEA (5.8 eq.), dry CH_2Cl_2/dry DMF, 30–35 °C, 40 h, argon; | method B: (i) CDI (1.2 eq.), dry THF, 28–30 °C, 1 h, argon; (ii) $PhCH_2ONH_2$·HCl (1.2 eq.), TEA (1.82 eq.), 28–30 °C, 24 h, argon; (f) H_2, Pd/C 10%, EtOH/AcOEt 3 : 1, 50–55 psi, 40–45 °C, 3 h. C) Methyl esters obtained because of unexpected transesterification reaction (pink frames).

increased the activity by 1.5 times (EC_{50} **17** = 0.38 μM) and benzocycloheptane by 6 times (EC_{50} **18** = 0.10 μM).

Moreover, *N*-methyl substitution on the hydantoin ring had a favorable effect on the antiviral activity, but only in the context of the indane- and tetralin-substituted analogues (EC_{50} **16a** = 0.21 μM; EC_{50} **17a** = 0.21 μM). The *N*-methylated analogue **18a** exhibited potency similar (in the order of 0.1 μM) to the parent compound **18**. The same trend was observed for the *N*-benzyl counterparts **16b** and **17b**, which were found to be 4 and 5.5 times more potent than their parent compounds **16** and **17**, respectively, whereas compound **18b** was equipotent (EC_{50} **18b** = 0.12 μM) to the NH and *N*-methyl congeners (EC_{50} **18** = 0.10 μM and EC_{50} **18a** = 0.11 μM, respectively). The increased activity of the compounds in HCV genotype 4a, as compared to the other genotypes, resulted in higher SI values, which ranged from >345 to 1984 for the NH analogues **16**, **17** and **18**. As for the *N*-methylated analogues, the most selective were **17a** (SI 682) and **18a** (SI 1015). Finally, out of all compounds, the most promising appeared to be **18**, whose SI values were significantly high: 794, 2480 and 1984 for genotypes 1b, 3a and 4a, respectively.

Validation of compounds 17a and 18 activity with additional assays. The inhibition profile of the most potent and safe compounds from the tetralin and benzocycloheptane groups, as measured by luciferase assay, was confirmed by determining viral RNA and NS5A protein levels. As the compounds showed higher activity against HCV genotype 4, Huh7.5-4a replicon cells were used for validating activity. Specifically, cells were treated with serial dilutions of compounds **17a** or **18**, or the solvent DMSO (control) and viral RNA was quantified by reverse transcription-quantitative polymerase chain reaction (RT-qPCR) whereas NS5A was evaluated by indirect immunofluorescence. We observed that

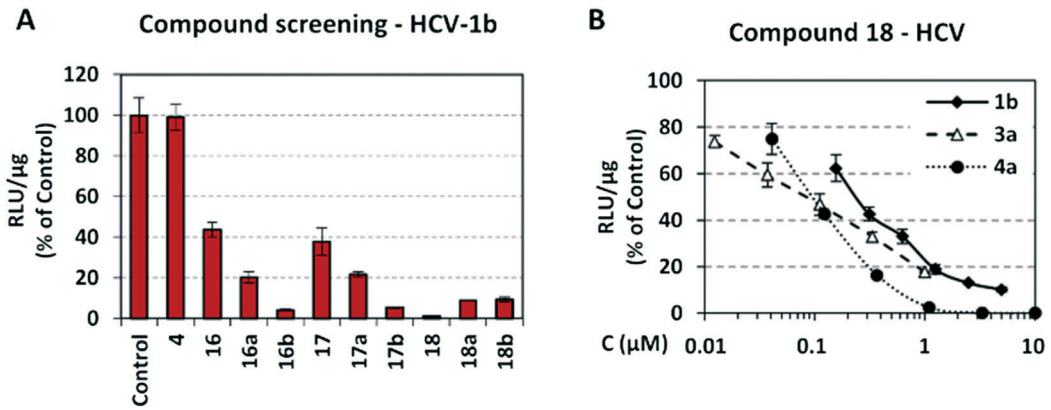

Fig. 4 A) Screening of compounds against HCV genotype 1b replication. Huh5-2 cells, harboring HCV genotype 1b (Con1) subgenomic replicon, were seeded at 30% confluency and treated for 72 h with the compounds at 3 μM. B) Activity of compound **18**, against HCV genotype 1b, 3a and 4a RNA replication, using dose–response curve analysis. Huh5-2, Huh7.5-3a and Huh7.5-4a cells, harboring subgenomic replicons of HCV genotype 1b (Con1), 3a (S52) or 4a (ED43), respectively, were seeded at 30% confluency and treated for 72 h with serial dilutions of **18**. In both A and B, as a marker of viral RNA replication, firefly luciferase activity was determined and calculated as relative light units (RLU) per μg of total protein. Values obtained with compound-treated cells were expressed as percentage of those obtained with cells treated with the solvent DMSO (control). Bars represent mean values obtained from three separate experiments in triplicate. Error bars represent standard deviation (SD).

compounds **17a** and **18** caused a reduction in HCV RNA replication (Fig. 5A), with EC_{50}s similar to those calculated on the basis of virus-derived luciferase activity (Table 1). Consistent results were obtained by indirect immunofluorescence analysis of HCV NS5A in Huh7.5-4a replicon cells treated with compound **18**, which were best visible at high compound concentration (Fig. 5B). Nuclei were stained with propidium iodide (PI) as a cell viability control.

Activity of the compounds against DENV. Taking into account the broad activity of the compounds against different HCV genotypes, they were also tested against the closely related DENV. Both HCV and DENV belong to the same family (*Flaviviridae*) and express metalloenzymes, which are potential targets of our compounds. To examine the anti-DENV activity of the non-substituted analogues (**16**, **17** and **18**), we determined viral replication-derived luciferase activity in Huh7-D2 stable cell line containing the subgenomic replicon of DENV serotype 2 (strain 16681). Interestingly, the order of activity obtained with **16**, **17** and **18** was the same when they were tested against DENV. Compound **16** exhibited the lowest inhibitory activity (EC_{50} = 96.34 μM), which was progressively increased along with the bulkiness of the spiro-substituent, resulting in an EC_{50} value of 16.29 μM for analogue **18**.

Trypanocidal assays

Activity of the compounds against T. brucei. Acetohydroxamic acid derivatives exhibited considerable trypanocidal activity against *T. brucei*, with EC_{50}s ranging from 0.013 to 1.91 μM. Compounds **18b** and **17b** were the most potent against African trypanosomes with low nanomolar EC_{50} values (13 nM and 50 nM respectively, Table 2), while hydroxamates **16b**, **17b** and **18b** were also significantly active against *T. cruzi* epimastigotes, with EC_{50} values in the low micromolar range.

Changing the indane ring in structure **16** with the tetralin ring decreased the activity, with the EC_{50} value of **17** being 1.5-fold higher (EC_{50} = 0.71 μM). Somewhat surprisingly, the replacement of indane by benzocycloheptane led to compound **18**, which was almost equipotent to lead compound **16** (EC_{50} **16** = 0.44 μM; EC_{50} **18** = 0.40 μM). These molecules appeared to confer a beneficial effect on the trypanocidal potency, with respect to the structurally related cycloheptane spiro-substituted 2,6-DKP analogue **II** (EC_{50} = 1.87 μM),[57] indicating that the fused bicyclic systems that were used as substituents at position 4 of the hydantoin core were a favorable structural modification.

Methyl substitution on the amide nitrogen atom of the respective 2,4-diketoimidazolidine residue of the parent compound **18** led to a 2-fold increase in potency for the benzocycloheptane substituted analogue **18a**. On the other hand, incorporation of a methyl substituent in **16** and **17**, lowered the activity observed in the *N*-methylated analogues **16a** and **17a**, with EC_{50} values 1.22 μM and 1.91 μM respectively. They were almost 3 times less potent than the corresponding NH-analogues (Table 2).

Addition of the bulky hydrophobic benzyl substituent to the same nitrogen atom of the hydantoin scaffold yielded analogues that were extremely potent against *T. brucei*, as exemplified by compounds **16b**, **17b** and **18b** (Table 2). Their activities were respectively 4.5, 14 and 31 times higher than the parent compounds **16**, **17** and **18**. All the *N*-benzylated analogues retained high potency, with EC_{50} values ranging between 13 and 101 nM (Table 2). It is noteworthy that the incorporation of a benzyl group in the corresponding non-substituted precursors **16**, **17** and **18** progressively increased activity against *T. brucei in vitro*. This enhanced potency of analogues **16b**, **17b** and **18b** reflects the strongly favorable stereoelectronic and hydrophobic effects exerted by the benzyl substituent in the binding site.

The cytotoxicity of all target compounds against mammalian cells was determined using the rat skeletal myoblast L6

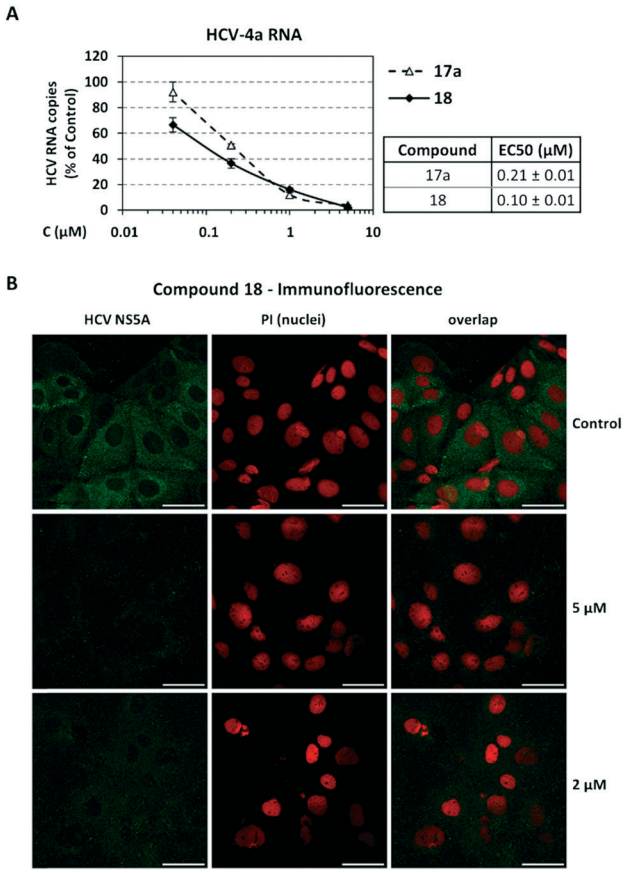

Fig. 5 Inhibitory effect of compounds on HCV RNA levels and protein expression in a subgenomic HCV Con1 replicon assay. A) Quantification of (+) strand HCV RNA by RT-qPCR in Huh7.5-4a replicon cells treated with serial dilutions of compounds **17a**, **18** or the solvent DMSO. Values from compound-treated cells are expressed as percentage of those obtained with cells that received the solvent (control). mRNA levels of the housekeeping gene YWHAZ were used for normalization. B) Indirect immunofluorescence for NS5A (left panels) in Huh7.5-4a replicon cells, treated with serial dilutions of compound **18** or the solvent DMSO. Nuclei were stained with propidium iodide (PI; middle panels). Merged images are shown at the right. Bar, 50 μm.

cell line. Notably, the non-substituted analogues **16**, **17** and **18** displayed very low cytotoxicity against mammalian cells, having CC_{50}s in the 125–419 μM range, thus resulting in remarkable selectivity indices, which varied from 313 (**18**) to 609 (**16**). In general, as in the case of HCV, it was observed that the incorporation of an alkyl substituent onto the amide nitrogen atom progressively increased the cytotoxicity of the compounds, with the exception of compound **16a** (CC_{50} = 550 μM, SI 451). Finally, the acetohydroxamic acid derivative **18b**, which had the highest activity against *T. brucei* (EC_{50} = 0.013 μM) displayed a very good selectivity (SI 604), despite the benzyl substitution.

Activity of the compounds against T. cruzi. Compounds were also tested against cultured *T. cruzi* epimastigotes, with EC_{50} values at submicromolar to micromolar levels (0.49–27.6 μM) (Table 2). Acetohydroxamic acid derivatives with a substituent on the amide nitrogen atom were able to inhibit parasite growth, an effect that was not observed with the non-substituted derivatives. More specifically, compounds **16**, **17** and **18** exhibited no activity at the highest concentration tested (30 μM), whereas the *N*-methylated analogues showed medium inhibitory activity (EC_{50} **17a** = 27.6 μM; EC_{50} **18a** = 10.6 μM), with the only exception being analogue **16a**. It is of great importance that the incorporation of a benzyl group resulted in unexpectedly potent analogues. The EC_{50}s obtained ranged from 0.49 μM for the bulkier analogue **18b** to 1.70 μM for the indane analogue **16b**, indicating the positive effect of increasing the bulkiness and lipophilicity of the compounds, a pattern also observed in *T. brucei* sp. Interestingly, activity of the *N*-benzylated analogue **18b** was 21.5-fold higher than the *N*-methylated counterpart **18a**. For the respective tetralin analogue **17b**, this increase in potency was 29 times higher. Finally, the absence of the acetohydroxamic acid moiety was detrimental for the activity against bloodstream form *T. brucei* and *T. cruzi* epimastigotes (Table 2), suggesting that the hydroxamic acid unit is essential also for the trypanocidal activity.

Concerning the physicochemical parameters of the prepared analogues, enhanced lipophilicity quantified by calculated log *D* values seems to be important to their bioactivity, and in most cases beneficial in terms of their capacity as drug leads. Conversely, pK_a values of the various analogues do not demonstrate significant difference and thus they do not appear to contribute to the observed structure–activity relationships.

Biological evaluation indicates that metalloproteins may constitute the targets of the acetohydroxamic acid-based analogues described herein. However, binding and pulldown assays will be helpful to fully rationalize the observed bioactivity and determine the exact molecular targets of the novel analogues, thus facilitating structure-based design of metalloenzyme inhibitors.

Conclusions

In summary, despite the small overlapping degree between the starting frameworks **I** and **II**, we have successfully designed and synthesized compounds with dual activity, by merging two distinct scaffolds into a single chemical entity. The framework combination strategy involved the integration of structural elements from indole–flutimide analogues, exhibiting antiviral potency, with spiro carbocyclic 2,6-DKP acetohydroxamic acid-based trypanocidal agents, in order to achieve both activities into a single lead molecule. The novel bicyclic substituted hydantoin analogues not only exhibited individually improved antiviral and antiparasitic activity compared to analogues **I** and **II**, but also demonstrated exceptional inhibitory activity against different HCV genotypes (1b, 3a, 4a) and DENV, as well the two *Trypanosoma* species (*T. brucei*, *T. cruzi*). Structure–activity relationships deduced from the biological results suggest that the increased size of the spiro-substituent generally favors inhibitory activity towards the targets of interest. Moreover, activity is enhanced upon

increasing the lipophilicity of the compounds, particularly *via* introduction of a methyl- or benzyl-substituent at the amide nitrogen atom of the hydantoin ring. In fact, the results suggest that increasing the bulkiness of the substituent improves rather than retards activity. Along with the lipophilicity, the acetohydroxamic acid moiety, capable of chelating active site metal ion(s), is an indispensable component of this class of inhibitors, since removal of this functional group from the imidic nitrogen atom caused a dramatic loss of activity. Finally, the remarkable selectivity indices observed for most of the tested analogues indicate that the novel scaffold of an appropriately substituted hydantoin ring and a metal binding moiety may be the key to unlock multiple pathogen inhibition, as a successful strategy for producing multifunctional drugs.

Experimental

Chemistry

Experimental methods. During the conduct of the experimental part of the present study were used the following materials, apparatuses and techniques. Melting points were determined using a Büchi capillary apparatus and are uncorrected. NMR experiments were performed to elucidate the structure and determine the purity of the newly synthesized compounds. ^{1}H NMR and 2D NMR spectra (COSY, HSQC, HSQC-DEPT and HMBC) were recorded on a Bruker DRX400 spectrometer (400.13 MHz, ^{1}H NMR) and a Bruker Ultrashield™ Plus Avance III 600 spectrometer (600.11 MHz, ^{1}H NMR). ^{13}C NMR and DEPT NMR spectra were recorded on a Bruker Avance 200 spectrometer (50.32 MHz, ^{13}C NMR) and a Bruker Ultrashield™ Plus Avance III 600 spectrometer (150.9 MHz, ^{13}C NMR). Chemical shifts δ (delta) are reported in parts per million (ppm) downfield from the NMR solvent, with the tetramethylsilane or solvent (DMSO-d_6) as internal standard. Data processing including Fourier transformation, baseline correction, phasing, peak peaking and integrations were performed using MestReNova software v.12.0.0. Splitting patterns are designated as follows: s, singlet; br s, broad singlet; d, doublet; br d, broad doublet; t, triplet; q, quartet; dd, doublet of doublets; ddd, doublet of doublets of doublets; dddd, doublet of doublets of doublets of doublets; ddddd, doublet of doublets of doublets of doublets of doublets; dt, doublet of triplets; dq, doublet of quartets; ddt, doublet of doublets of triplets; ddq, doublet of doublets of quartets; dtt, doublet of triplets of triplets; dqt, doublet of quartets of triplets; ddtd, doublet of doublets of triplets of doublets; td, triplet of doublets; tdd, triplet of doublets of doublets; qt, quartet of triplets; m, multiplet; complex m, complex multiplet. Coupling constants (J) are expressed in units of Hertz (Hz). The spectra were recorded at 293 K (20 °C) unless otherwise specified. The solvents used to obtain the spectra were: deuterated chloroform, $CDCl_3$ (s, 7.26 ppm, ^{1}H NMR; t, 77.16 ppm, ^{13}C NMR), deuterated dimethyl sulfoxide, DMSO-d_6 (quin, 2.50 ppm, ^{1}H NMR; septet, 39.52 ppm, ^{13}C NMR) and deuterated methanol, MeOD-d_4 (quin, 3.31 ppm, ^{1}H NMR; septet, 49.00 ppm, ^{13}C NMR). Analytical thin-layer chromatography (TLC) was used to monitor the progress of the reactions, as well as to authenticate the compounds. TLCs were conducted on, precoated with normal-phase silica gel, aluminium sheets (Silica gel 60 F_{254}, Merck) (layer thickness 0.2 mm). Developed plates were examined under a UV light source, at wavelengths of 254 nm and 365 nm, or after being stained by iodine vapors. The Retention factor (R_f) of the newly synthesized compounds, that equals to the distance migrated over the total distance covered by the solvent, was also measured on the chromatoplates. Column chromatography technique was used to isolate the desired compounds from by-products of reactions, and it was carried out using elution solvents of increasing polarity in a stationary phase of SiO_2 (Silica gel 60, 40–63 μm, 230–400 mesh ASTM, Silica flash). Column packing was done using the slurry method, while the mixtures to be analyzed were loaded using either the technique of dry deposition, or as a solution in the first eluent where this was possible. Elemental analyses (C, H, N) were performed by the Service Central de Microanalyse at CNRS (France), and were within ±0.4% of the theoretical values. Elemental analysis results for the tested compounds correspond to >95% purity. The commercial reagents were purchased from Alfa Aesar, Sigma-Aldrich, and Merck, and were used without further purification, except for the benzyl bromoacetate. This reagent was purified by fractional distillation *in vacuo* prior to use. Organic solvents used were in the highest purity, and when necessary, were dried by the standard methods. Solvent and reagent abbreviations: THF, tetrahydrofuran; DMF, *N*,*N*-dimethylformamide; Et_2O, diethyl ether; AcOEt, ethyl acetate; EtOH, ethanol; MeOH, methanol; EDCI·HCl, *N*-(3-dimethylaminopropyl)-*N*′-ethylcarbodiimide hydrochloride; HOBt, 1-hydroxybenzotriazole hydrate; CDI, 1,1′-carbonyldiimidazole; TEA, triethylamine.

General experimental procedures

General experimental procedure for the preparation of carboxylic acids 10–12, 10a–12a and 10b–12b. A solution of the appropriate benzyl ester **7–9**, **7a–9a** and **7b–9b** (2.0 mmol) in a mixture of EtOH/AcOEt 3 : 1 (40 mL) was hydrogenated for 3 h at 40–45 °C and 50–55 psi pressure, in the presence of Pd/C (10 wt%) as a catalyst. The catalyst was filtered off, washed with portions of hot MeOH (3 × 15 mL) and the combined filtrates were evaporated under reduced pressure to yield the corresponding carboxylic acids **10–12**, **10a–12a** and **10b–12b**.

General experimental procedure for the preparation of *N*-(phenylmethoxy)acetamides 13–15, 13a–15a and 13b–15b

Method A. To a solution of the appropriate carboxylic acid (**10**, **12**, **12b**) (2.0 mmol, 1.0 eq.) in 20 mL dry CH_2Cl_2/dry DMF (4 : 1), EDCI·HCl (2.4 mmol, 1.2 eq.), HOBt (2.4 mmol, 1.2 eq., 80% monohydrate), *O*-benzylhydroxylamine hydrochloride (2.4 mmol, 1.2 eq.) and TEA (11.6 mmol, 5.8 eq.) were added sequentially. The reaction mixture was stirred for 40 h, at 30–35 °C under argon. After removal of CH_2Cl_2 under reduced pressure, ice-water was added (40 mL)

and the mixture was extracted with AcOEt (4 × 40 mL). The combined organic layers were washed with H_2O (3 × 70 mL) and brine (2 × 70 mL), dried over anh. Na_2SO_4 and evaporated *in vacuo*. The crude residue was purified by column chromatography on silica gel using a mixture of CH_2Cl_2/AcOEt and AcOEt as eluents to afford the desired amides (**13**, **15**, **15b** respectively).

Method B. The appropriate carboxylic acid (**11**, **10a–12a**, **10b**, **11b**) (2.0 mmol, 1.0 eq.) was treated with CDI (2.4 mmol, 1.2 eq.) in dry THF (26 mL) and the mixture was stirred for 1 h, at 28–30 °C under argon. Then, *O*-benzylhydroxylamine hydrochloride (2.4 mmol, 1.2 eq.) and TEA (3.64 mmol, 1.82 eq.) were added successively, and the stirring was continued for 24 h, at 28–30 °C under Ar. After removal of the solvent *in vacuo*, the reaction mixture was quenched with ice-water (40 mL) and extracted with AcOEt (4 × 40 mL). The combined organic phases were washed with H_2O (3 × 70 mL) and brine (2 × 70 mL), dried with anh. Na_2SO_4 and evaporated under reduced pressure. The crude residue was purified by column chromatography on silica gel using a mixture of CH_2Cl_2/AcOEt and AcOEt as eluents to afford the desired amides (**14**, **13a–15a**, **13b**, **14b** respectively).

General experimental procedure for the preparation of the hydroxamic acids 16–18, 16a–18a and 16b–18b. 10 wt% Pd on charcoal was added to a solution of the appropriate *O*-benzyl hydroxamate (**13–15**, **13a–15a**, **13b–15b**) (1.0 mmol) in a mixture of EtOH/AcOEt 3 : 1 (40 mL). After 3 h of shaking under an atmosphere of 50–55 psi hydrogen, at 40–45 °C, the catalyst was removed by filtration and washed with hot MeOH (3 × 15 mL). The combined filtrates were concentrated to dryness under reduced pressure to afford the title acetohydroxamic acid analogues (**16–18**, **16a–18a** and **16b–18b** respectively).

General *N*-benzylation procedure for the preparation of analogues 7b–9b. The appropriate benzyl ester (**7–9**) (2.6 mmol, 1.0 eq.) was dissolved in 12 mL dry DMF and was treated with small portions of NaH (3.12 mmol, 1.2 eq., 60% dispersion in mineral oil) under ice-cooling. After 15 min of stirring at r.t. under argon, benzyl bromide was added dropwise (3.12 mmol, 1.2 eq.). After 7 days of stirring at 60 °C, under argon, the mixture was poured into 120 mL ice-water and extracted with AcOEt (3 × 90 mL). The combined organic layers were washed with H_2O (3 × 150 mL) and brine (2 × 150 mL), dried over anh. Na_2SO_4 and the solvent was evaporated *in vacuo*. The resulting oily residue was chromatographed on silica gel column to afford the title *N*-benzylated products **7b–9b**.

2-(2,5-Dioxo-2′,3′-dihydrospiro[imidazolidine-4,1′-inden]-1-yl)acetic acid (10). Prepared from benzyl ester **7** (420 mg, 1.2 mmol) by catalytic hydrogenolysis in a mixture of EtOH/AcOEt 3 : 1 (24 mL), following the previously described general procedure for the preparation of carboxylic acids. Evaporation of the solvents under reduced pressure afforded the title compound **10** as a white crystalline solid (310 mg, almost quantitative yield); mp 237–239 °C (from AcOEt/*n*-pentane), R_f = 0.06 (AcOEt). ^{1}H NMR (600.11 MHz, DMSO-d_6) δ (ppm) 2.22 (dt, 1H, J_1 = 13.3 Hz, J_2 = 7.8 Hz, $H_{2'}$), 2.55 (dt, 1H, J_1 = 13.2 Hz, J_2 = 6.5 Hz, $H_{2'}$), 3.05 (t, 2H, J = 7.2 Hz, $H_{3'}$), 4.07–4.15 (q, AB, 2H, J_{AB} = 17.5 Hz, NCH_2COOH), 7.19 (d, 1H, J = 7.5 Hz, $H_{7'}$), 7.26 (tdd, 1H, J_1 = 7.0 Hz, J_2 = 1.9 Hz, J_3 = 1.0 Hz, $H_{6'}$), 7.33 (td, 1H, J_1 = 7.5 Hz, J_2 = 1.2 Hz, $H_{5'}$), 7.34–7.36 (m, 1H, $H_{4'}$), 8.84 (s, 1H, H_3), 13.12 (br s, 1H, NCH$_2$COO*H*); ^{13}C NMR (150.9 MHz, DMSO-d_6) δ (ppm) 29.7 ($C_{3'}$), 36.0 ($C_{2'}$), 39.1 (N*C*H$_2$COOH), 70.8 ($C_{1'}$/C_4), 123.1 ($C_{7'}$), 125.0 ($C_{4'}$), 127.0 ($C_{6'}$), 129.0 ($C_{5'}$), 141.0 ($C_{7a'}$), 143.9 ($C_{3a'}$), 155.2 (C_2═O), 168.7 (NCH$_2$*C*OOH), 175.2 (C_5═O). Found: C, 60.08; H, 4.70; N, 10.79. Calc. for $C_{13}H_{12}N_2O_4$: C, 60.00; H, 4.65; N, 10.76%.

***N*-(Phenylmethoxy)-2-(2,5-dioxo-2′,3′-dihydrospiro-[imidazolidine-4,1′-inden]-1-yl)acetamide (13).** Carboxylic acid **10** (260 mg, 1.0 mmol) was treated with EDCI·HCl (230 mg, 1.2 mmol), HOBt (203 mg, 1.2 mmol, 80% monohydrate), *O*-benzylhydroxylamine hydrochloride (192 mg, 1.2 mmol) and TEA (587 mg, 5.8 mmol) in 10 mL dry CH_2Cl_2/dry DMF (4 : 1) following the general procedure for the preparation of *O*-benzyl hydroxamates (Method A). After removal of CH_2Cl_2 under reduced pressure, the reaction mixture was poured into 20 mL ice-water and extracted with AcOEt (4 × 20 mL). The combined organic layers were washed with H_2O (3 × 35 mL) and brine (2 × 35 mL), dried over Na_2SO_4 and concentrated to dryness *in vacuo*. The oily pale-yellow residue was purified by column chromatography on silica gel eluting first with CH_2Cl_2/AcOEt 8 : 1, 5 : 1 and then AcOEt to give the corresponding *O*-benzyl hydroxamate **13** as a white foamy solid, which strongly binds the eluting solvents. Removal of the entrapped solvents upon drying under high vacuum and treatment with *n*-pentane at 0 °C gave **13** as a white crystalline solid (260 mg, 71%); mp 154–156 °C (AcOEt/*n*-pentane), R_f = 0.06 (from CH_2Cl_2/AcOEt 8 : 1). ^{1}H NMR (600.11 MHz, DMSO-d_6) δ (ppm) 2.22 (dt, 1H, J_1 = 13.5 Hz, J_2 = 7.7 Hz, $H_{2'}$), 2.57 (dt, 1H, J_1 = 13.1 Hz, J_2 = 6.6 Hz, $H_{2'}$), 3.05 (t, 2H, J = 7.1 Hz, $H_{3'}$), 3.92–4.01 (q, AB, 1.55H, J_{AB} = 16.3 Hz, NCH_2CO), 4.25 (br s, 0.3H, NCH_2CO), 4.81, 4.86 (s + s, 2H, OCH_2Ph), 7.25–7.30 (m, 2H, $H_{6'}$, $H_{7'}$), 7.31–7.35 (m, 2H, $H_{4'}$, $H_{5'}$), 7.35–7.47 (m, 5H, $H_{2''}$, $H_{3''}$, $H_{4''}$, $H_{5''}$, $H_{6''}$), 8.81 (s, 1H, H_3), 11.02 (s, 0.1H, CON*H*OCH$_2$Ph), 11.39 (s, 0.7H, CON*H*OCH$_2$Ph); ^{13}C NMR (150.9 MHz, DMSO-d_6) δ (ppm) 29.7 ($C_{3'}$), 36.0 ($C_{2'}$), 38.0 (N*C*H$_2$CO), 70.8 ($C_{1'}$/C_4), 77.0 (O*C*H$_2$Ph), 123.3 ($C_{7'}$), 124.9 ($C_{4'}$), 127.0 ($C_{6'}$), 128.3 ($C_{3''}$, $C_{4''}$, $C_{5''}$), 128.8 ($C_{2''}$, $C_{6''}$), 129.0 ($C_{5'}$), 135.8 ($C_{1''}$), 141.1 ($C_{7a'}$), 143.9 ($C_{3a'}$), 155.3 (C_2═O), 163.6 (*C*ONHOCH$_2$Ph), 175.4 (C_5═O). Found: C, 65.69; H, 5.30; N, 11.53. Calc. for $C_{20}H_{19}N_3O_4$: C, 65.74; H, 5.24; N, 11.50%.

***N*-Hydroxy-2-(2,5-dioxo-2′,3′-dihydrospiro[imidazolidine-4,1′-inden]-1-yl)acetamide (16).** A solution of the appropriate *O*-benzyl hydroxamate **13** (200 mg, 0.55 mmol) in a mixture of EtOH/AcOEt (3 : 1, 22 mL) was hydrogenated following the general procedure described above for the preparation of acetohydroxamic acids. Evaporation of the solvents *in vacuo* yielded the title compound **16** as a white foamy solid, which strongly binds the aforementioned solvents. Removal of the entrapped solvents upon drying under high vacuum gave **16** as a glass solid, which was further crystallized upon

treatment with *n*-pentane-dry Et_2O 5 : 1 under ice-cooling (150 mg, almost quantitative yield); mp 179–182 °C (from AcOEt/*n*-pentane-dry Et_2O), R_f = 0.29 (AcOEt). This compound appeared in the ^1H and ^{13}C NMR spectra as a mixture of *E*/*Z* conformers. ^1H NMR (600.11 MHz, DMSO-d_6) δ (ppm) 2.22 (dt, 1H, J_1 = 13.4 Hz, J_2 = 7.5 Hz, $H_{2'}$), 2.56 (ddd, 1H, J_1 = 13.4 Hz, J_2 = 7.5 Hz, J_3 = 6.0 Hz, $H_{2'}$), 3.04 (ddd, 2H, J_1 = 8.2 Hz, J_2 = 6.5 Hz, J_3 = 2.4 Hz, $H_{3'}$), 3.91–4.00 (q, AB, 1.5H, J_{AB} = 16.5 Hz, NCH_2CO, *E*-isomer), 4.20–4.29 (q, AB, 0.45H, J_{AB} = 17.5 Hz, NCH_2CO, *Z*-isomer), 7.23–7.35 (complex m, 4H, $H_{4'}$, $H_{5'}$, $H_{6'}$, $H_{7'}$), 8.73 (s, 0.1H, H_3), 8.76, 8.77 (s + s, 0.9H, H_3), 8.95 (s, 0.6H, CH_2CONHO*H*, *E*-isomer), 9.33 (s, 0.2H, NCH_2-CONHO*H*, *Z*-isomer), 10.29 (s, 0.2H, NCH_2CON*H*OH, *Z*-isomer), 10.72 (s, 0.6H, CH_2CON*H*OH, *E*-isomer); ^{13}C NMR (150.9 MHz, DMSO-d_6) δ (ppm) 29.8 ($C_{3'}$), 36.0, 36.1 ($C_{2'}$), 38.0 (N*C*H_2CO, *E*-isomer), 38.5 (N*C*H_2CO, *Z*-isomer), 70.8 ($C_{1'}$/C_4), 123.4 ($C_{7'}$), 124.9 ($C_{4'}$), 127.0 ($C_{6'}$), 129.0 ($C_{5'}$), 141.3 ($C_{7a'}$), 143.9 ($C_{3a'}$), 155.4 (C_2═O, *E*-isomer), 155.6 (C_2═O, *Z*-isomer), 163.3 (NCH_2*C*O, *E*-isomer), 168.7 (NCH_2*C*O, *Z*-isomer), 175.5 (C_5═O, *E*-isomer), 175.7 (C_5═O, *Z*-isomer). Found: C, 56.78; H, 4.81; N, 15.30. Calc. for $C_{13}H_{13}N_3O_4$: C, 56.72; H, 4.75; N, 15.27%.

2-(3-Methyl-2,5-dioxo-2′,3′-dihydrospiro[imidazolidine-4,1′-inden]-1-yl)acetic acid (10a). It was prepared by hydrogenolysis of the corresponding benzyl ester **7a** (320 mg, 0.88 mmol) in a mixture of 18 mL EtOH/AcOEt (3 : 1), following the general procedure for the preparation of carboxylic acids. After removal of the solvent under reduced pressure, the title compound **10a** was obtained as a white crystalline solid (240 mg, almost quantitative yield); mp 203–205 °C (melted gradually from 198 °C) (AcOEt/*n*-pentane), R_f = 0.24 (AcOEt). ^1H NMR (400.13 MHz, MeOD-d_4) δ (ppm) 2.40 (ddd, 1H, J_1 = 13.9 Hz, J_2 = 8.4 Hz, J_3 = 6.8 Hz, $H_{2'}$), 2.56 (ddd, 1H, J_1 = 14.0 Hz, J_2 = 8.3 Hz, J_3 = 5.7 Hz, $H_{2'}$), 2.69 (s, 3H, NCH_3), 3.07–3.22 (m, 2H, $H_{3'}$), 4.21–4.34 (q, AB, 2H, J_{AB} = 17.6 Hz, NCH_2COOH), 5.13 (br s, 1H, NCH_2COO*H*), 7.20 (d, 1H, *J* = 7.3 Hz, $H_{7'}$), 7.22–7.29 (m, 1H, $H_{6'}$), 7.31–7.38 (m, 2H, $H_{4'}$, $H_{5'}$); ^{13}C NMR (50.32 MHz, MeOD-d_4) δ (ppm) 25.4 (N*C*H_3), 31.4 ($C_{3'}$), 33.5 ($C_{2'}$), 40.4 (N*C*H_2COOH), 76.5 ($C_{1'}$/C_4), 124.5 ($C_{7'}$), 126.4 ($C_{4'}$), 128.4 ($C_{6'}$), 130.9 ($C_{5'}$), 139.0 ($C_{7a'}$), 146.4 ($C_{3a'}$), 156.6 (C_2═O), 170.3 (NCH_2*C*OOH), 176.6 (C_5═O). Found: C, 61.29; H, 5.21; N, 10.28. Calc. for $C_{14}H_{14}N_2O_4$: C, 61.31; H, 5.15; N, 10.21%.

***N*-(Phenylmethoxy)-2-(3-methyl-2,5-dioxo-2′,3′-dihydrospiro-[imidazolidine-4,1′-inden]-1-yl)acetamide (13a).** Using the general procedure for the preparation of *N*-(phelylmethoxy)acetamides (Method B), the carboxylic acid precursor **10a** (200 mg, 0.73 mmol) was treated with CDI (143 mg, 0.88 mmol), *O*-benzylhydroxylamine hydrochloride (140 mg, 0.88 mmol) and TEA (135 mg, 1.33 mmol) in dry THF (9 mL). After removal of the solvent *in vacuo*, the reaction mixture was quenched with 15 mL ice-water and extracted with AcOEt (4 × 15 mL). The combined organic phases were washed with H_2O (3 × 25 mL) and brine (2 × 25 mL), dried over anh. Na_2SO_4 and evaporated under reduced pressure. The pale-yellow viscous oily residue was purified by column chromatography on silica gel using CH_2Cl_2, CH_2Cl_2/AcOEt 20 : 1, 10 : 1 and AcOEt as eluents to afford the corresponding *O*-benzyl hydroxamate **13a** as a colorless oil, which was further crystallized to a white crystalline solid by treatment with *n*-pentane under ice-cooling (210 mg, 76%); mp 108–110 °C (from AcOEt/*n*-pentane-dry Et_2O), R_f = 0.21 (CH_2Cl_2/AcOEt 8 : 1). ^1H NMR (600.11 MHz, DMSO-d_6) δ (ppm) 2.41 (ddd, 1H, J_1 = 14.4 Hz, J_2 = 8.5 Hz, J_3 = 6.7 Hz, $H_{2'}$), 2.48 (ddd, 1H, J_1 = 14.3 Hz, J_2 = 8.3 Hz, J_3 = 6.0 Hz, $H_{2'}$), 2.62 (s, 3H, NCH_3), 3.05–3.16 (m, 2H, $H_{3'}$), 3.96–4.06 (q, AB, 1.6H, J_{AB} = 16.2 Hz, NCH_2CO), 4.27 (br s, 0.3H, NCH_2CO), 4.81, 4.86 (s + s, 2H, OCH_2Ph), 7.22 (d, 1H, *J* = 7.6 Hz, $H_{7'}$), 7.29 (t, 1H, *J* = 7.2 Hz, $H_{6'}$), 7.33–7.47 (m, 7H, $H_{4'}$, $H_{5'}$, $H_{2''}$, $H_{3''}$, $H_{4''}$, $H_{5''}$, $H_{6''}$), 11.06 (s, 0.1H, CON*H*OCH_2Ph), 11.40 (s, 0.7H, CON*H*OCH_2Ph); ^{13}C NMR (150.9 MHz, DMSO-d_6) δ (ppm) 24.7 (N*C*H_3), 30.0 ($C_{3'}$), 32.1 ($C_{2'}$), 38.4 (N*C*H_2CO), 74.3 ($C_{1'}$/C_4), 77.0 (O*C*H_2Ph), 123.4 ($C_{7'}$), 125.2 ($C_{4'}$), 127.2 ($C_{6'}$), 128.3 ($C_{3''}$, $C_{4''}$, $C_{5''}$), 128.8 ($C_{2''}$, $C_{6''}$), 129.5 ($C_{5'}$), 135.7 ($C_{1''}$), 138.0 ($C_{7a'}$), 144.7 ($C_{3a'}$), 155.3 (C_2═O), 163.6 (*C*ONHOCH_2Ph), 175.4 (C_5═O). Found: C, 66.54; H, 5.61; N, 11.00. Calc. for $C_{21}H_{21}N_3O_4$: C, 66.48; H, 5.58; N, 11.08%.

***N*-Hydroxy-2-(3-methyl-2,5-dioxo-2′,3′-dihydrospiro-[imidazolidine-4,1′-inden]-1-yl)acetamide (16a).** A mixture of the *O*-benzyl hydroxamate **13a** (160 mg, 0.42 mmol) and Pd on charcoal (19 mg) in EtOH/AcOEt 3 : 1 (17 mL) was subjected to catalytic hydrogenolysis in exactly the same procedure described above for the preparation of the final compounds. Removal of the solvents under reduced pressure provided the acetohydroxamic acid **16a** as a white foamy solid. Crystallization of this product upon treatment with *n*-pentane-dry Et_2O under ice-cooling gave a white crystalline solid (120 mg, almost quantitative yield); mp melted gradually from 158 °C to 162 °C (AcOEt/*n*-pentane-dry Et_2O), R_f = 0.22 (from AcOEt). This compound exhibited distinct peaks attributed to each of the two *E*/*Z* conformers in the ^1H and ^{13}C NMR spectra. ^1H NMR (600.11 MHz, DMSO-d_6) δ (ppm) 2.40 (ddd, 1H, J_1 = 14.1 Hz, J_2 = 8.5 Hz, J_3 = 4.2 Hz, $H_{2'}$), 2.47 (ddd, 1H, J_1 = 14.1 Hz, J_2 = 8.2 Hz, J_3 = 4.0 Hz, $H_{2'}$), 2.61 (s, 3H, NCH_3), 3.04–3.16 (m, 2H, $H_{3'}$), 3.95–4.04 (q, AB, 1.5H, J_{AB} = 16.1 Hz, NCH_2CO, *E*-isomer), 4.24–4.33 (q, AB, 0.5H, J_{AB} = 17.3 Hz, NCH_2CO, *Z*-isomer), 7.23 (d, 1H, *J* = 7.8 Hz, $H_{7'}$), 7.27 (td, 1H, J_1 = 7.3 Hz, J_2 = 2.0 Hz, $H_{6'}$), 7.34–7.40 (m, 2H, $H_{4'}$, $H_{5'}$), 8.98 (s, 0.7H, CH_2CONHO*H*, *E*-isomer), 9.36 (s, 0.23H, NCH_2CONHO*H*, *Z*-isomer), 10.34 (s, 0.23H, NCH_2-CON*H*OH, *Z*-isomer), 10.75 (s, 0.7H, CH_2CON*H*OH, *E*-isomer); ^{13}C NMR (150.9 MHz, DMSO-d_6) δ (ppm) 24.8 (N*C*H_3), 30.1 ($C_{3'}$), 32.1 ($C_{2'}$), 38.5 (N*C*H_2CO, *E*-isomer), 39.0 (N*C*H_2CO, *Z*-isomer), 74.3 ($C_{1'}$/C_4), 123.5, 123.6 ($C_{7'}$), 125.2 ($C_{4'}$), 127.2 ($C_{6'}$), 129.5 ($C_{5'}$), 138.2 ($C_{7a'}$), 144.7 ($C_{3a'}$), 154.6 (C_2═O, *E*-isomer), 154.7 (C_2═O, *Z*-isomer), 163.2 (NCH_2*C*O, *E*-isomer), 168.6 (NCH_2*C*O, *Z*-isomer), 174.6 (C_5═O, *E*-isomer), 174.8 (C_5═O, *Z*-isomer). Found: C, 58.23; H, 5.26; N, 14.50. Calc. for $C_{14}H_{15}N_3O_4$: C, 58.13; H, 5.23; N, 14.53%.

Benzyl 2-(3-benzyl-2,5-dioxo-2′,3′-dihydrospiro-[imidazolidine-4,1′-inden]-1-yl)acetate (7b). A stirred solution of benzyl ester **7** (600 mg, 1.71 mmol) in dry DMF (7.6 mL) was treated with NaH (82 mg, 2.05 mmol, 60% dispersion in

mineral oil) and benzyl bromide (351 mg, 2.05 mmol) by employing the *N*-alkylation reaction described above. The reaction mixture was poured into an ice-water mixture (80 mL) and extracted with AcOEt (3 × 60 mL). The combined organic phases were washed with H_2O (3 × 100 mL) and brine (2 × 100 mL), dried over anh. Na_2SO_4 and evaporated under reduced pressure. The brownish-yellow crude oily residue was purified by silica gel column chromatography. CH_2Cl_2 was used as eluent to afford the target compound **7b** as a white crystalline solid (510 mg, 68%); mp 129–131 °C (from AcOEt/*n*-pentane), R_f = 0.76 (CH_2Cl_2/AcOEt 8 : 1). ^{1}H NMR (600.11 MHz, $CDCl_3$) δ (ppm) 2.05 (ddd, 1H, J_1 = 14.2 Hz, J_2 = 8.9 Hz, J_3 = 5.5 Hz, $H_{2'}$), 2.52 (ddd, 1H, J_1 = 13.8 Hz, J_2 = 9.1 Hz, J_3 = 5.6 Hz, $H_{2'}$), 2.84 (ddd, 1H, J_1 = 16.0 Hz, J_2 = 8.9 Hz, J_3 = 5.6 Hz, $H_{3'}$), 3.07 (ddd, 1H, J_1 = 15.9 Hz, J_2 = 9.1 Hz, J_3 = 5.5 Hz, $H_{3'}$), 3.81 (d, 1H, J = 15.9 Hz, NC*H*HPh), 4.41–4.49 (q, AB, 2H, J_{AB} = 17.3 Hz, NCH_2COO), 4.82 (d, 1H, J = 15.9 Hz, NCH*H*Ph), 5.20–5.26 (q, AB, 2H, J_{AB} = 12.1 Hz, OCH_2Ph), 7.06 (d, 1H, J = 7.7 Hz, $H_{7'}$), 7.10–7.13 (m, 2H, H_{2Bz}, H_{6Bz}), 7.14 (td, 1H, J_1 = 7.4 Hz, J_2 = 1.3 Hz, $H_{6'}$), 7.21–7.27 (complex m, 3H, H_{3Bz}, H_{4Bz}, H_{5Bz}), 7.28 (dt, 1H, J_1 = 7.5 Hz, J_2 = 1.1 Hz, $H_{4'}$), 7.31 (td, 1H, J_1 = 7.4 Hz, J_2 = 1.1 Hz, $H_{5'}$), 7.34–7.41 (m, 5H, $H_{2''}$, $H_{3''}$, $H_{4''}$, $H_{5''}$, $H_{6''}$); ^{13}C NMR (150.9 MHz, $CDCl_3$) δ (ppm) 30.7 ($C_{3'}$), 33.9 ($C_{2'}$), 40.1 (N*C*H_2COO), 44.1 (N*C*H_2Ph), 67.9 (COO*C*H_2Ph), 76.0 ($C_{1'}$/C_4), 124.0 ($C_{7'}$), 125.4 ($C_{4'}$), 127.7 (C_{2Bz}, C_{6Bz}), 127.8 ($C_{6'}$), 128.6 (C_{3Bz}, C_{5Bz}), 128.7 ($C_{2''}$, $C_{6''}$, C_{4Bz}), 128.76 ($C_{4''}$), 128.84 ($C_{3''}$, $C_{5''}$), 130.0 ($C_{5'}$), 135.0 ($C_{1''}$), 137.5 (C_{1Bz}), 137.9 ($C_{7a'}$), 145.1 ($C_{3a'}$), 155.7 (C_2═O), 167.3 (*C*OOCH$_2$Ph), 175.0 (C_5═O). Found: C, 73.66; H, 5.55; N, 6.30. Calc. for $C_{27}H_{24}N_2O_4$: C, 73.62; H, 5.49; N, 6.36%.

2-(3-Benzyl-2,5-dioxo-2′,3′-dihydrospiro[imidazolidine-4,1′-inden]-1-yl)acetic acid (10b). Prepared from benzyl ester **7b** (400 mg, 0.91 mmol) by catalytic hydrogenolysis in a mixture of 18 mL EtOH/AcOEt (3 : 1) following the procedure described for the preparation of the above-mentioned carboxylic acids. The desired compound **10b** was afforded as a glass solid, which was further crystallized upon treatment with *n*-pentane-dry Et_2O (5 : 1) under ice-cooling to give a white crystalline solid (316 mg, almost quantitative yield); mp 144–147 °C (from AcOEt/*n*-pentane), R_f = 0.22 (AcOEt). ^{1}H NMR (600.11 MHz, DMSO-d_6) δ (ppm) 2.14 (ddd, 1H, J_1 = 14.1 Hz, J_2 = 8.7 Hz, J_3 = 5.6 Hz, $H_{2'}$), 2.44 (ddd, 1H, J_1 = 14.5 Hz, J_2 = 8.9 Hz, J_3 = 5.9 Hz, $H_{2'}$), 2.93 (ddd, 1H, J_1 = 15.8 Hz, J_2 = 8.7 Hz, J_3 = 5.9 Hz, $H_{3'}$), 3.00 (ddd, 1H, J_1 = 15.0 Hz, J_2 = 8.9 Hz, J_3 = 5.6 Hz, $H_{3'}$), 3.96 (d, 1H, J = 16.3 Hz, NC*H*HPh), 4.19–4.27 (q, AB, 2H, J_{AB} = 17.4 Hz, NCH_2-COOH), 4.58 (d, 1H, J = 16.3 Hz, NCH*H*Ph), 7.07–7.14 (m, 3H, $H_{7'}$, H_{2Bz}, H_{6Bz}), 7.15–7.26 (complex m, 4H, $H_{6'}$, H_{3Bz}, H_{4Bz}, H_{5Bz}), 7.30–7.35 (m, 2H, $H_{4'}$, $H_{5'}$), 13.33 (br s, 1H, NCH$_2$COO*H*); ^{13}C NMR (150.9 MHz, DMSO-d_6) δ (ppm) 30.0 ($C_{3'}$), 33.0 ($C_{2'}$), 40.1 (N*C*H$_2$COOH), 43.2 (N*C*H$_2$Ph), 74.9 ($C_{1'}$/C_4), 123.6 ($C_{7'}$), 125.2 ($C_{4'}$), 127.1 ($C_{6'}$, C_{2Bz}, C_{4Bz}, C_{6Bz}), 128.2 (C_{3Bz}, C_{5Bz}), 129.5 ($C_{5'}$), 137.6 (C_{1Bz}), 138.3 ($C_{7a'}$), 144.7 ($C_{3a'}$), 155.1 (C_2═O), 168.7 (NCH$_2$*C*OOH), 174.3 (C_5═O). Found: C, 68.60; H, 5.14; N, 8.13. Calc. for $C_{20}H_{18}N_2O_4$: C, 68.56; H, 5.18; N, 8.00%.

***N*-(Phenylmethoxy)-2-(3-benzyl-2,5-dioxo-2′,3′-dihydrospiro-[imidazolidine-4,1′-inden]-1-yl)acetamide (13b).** Prepared from carboxylic acid **10b** (290 mg, 0.83 mmol) upon treatment with CDI (162 mg, 1.0 mmol), *O*-benzylhydroxylamine hydrochloride (160 mg, 1.00 mmol) and TEA (153 mg, 1.51 mmol) in dry THF (11 mL), following the general procedure for the synthesis of *O*-benzyl hydroxamates (Method B). After removal of THF under reduced pressure, the reaction mixture was quenched with 20 mL ice-water and extracted with AcOEt (4 × 20 mL). The combined organic layers were washed with H_2O (3 × 35 mL) and brine (2 × 35 mL), dried with anh. Na_2SO_4 and evaporated *in vacuo*. The resulting viscous oily residue was chromatographed on silica gel using CH_2Cl_2, CH_2Cl_2/AcOEt 20 : 1, 10 : 1 and AcOEt as eluents to give the corresponding *O*-benzyl hydroxamate **13b** as a glass solid. Crystallization of this material upon treatment with a *n*-pentane-dry Et_2O mixture (5 : 1) gave a white crystalline solid (310 mg, 82%); mp melted gradually from 60 °C to 78 °C (from AcOEt/*n*-pentane-dry Et_2O), R_f = 0.41 (CH_2Cl_2/AcOEt 8 : 1). ^{1}H NMR (600.11 MHz, DMSO-d_6) δ (ppm) 2.13 (ddd, 1H, J_1 = 14.0 Hz, J_2 = 8.6 Hz, J_3 = 5.3 Hz, $H_{2'}$), 2.45 (ddd, 1H, J_1 = 14.5 Hz, J_2 = 8.9 Hz, J_3 = 6.0 Hz, $H_{2'}$), 2.93 (ddd, 1H, J_1 = 15.8 Hz, J_2 = 8.6 Hz, J_3 = 6.0 Hz, $H_{3'}$), 2.99 (ddd, 1H, J_1 = 14.9 Hz, J_2 = 8.8 Hz, J_3 = 5.4 Hz, $H_{3'}$), 3.94 (d, 1H, J = 16.3 Hz, NC*H*HPh), 4.04–4.13 (q, AB, 1.65H, J_{AB} = 16.2 Hz, NCH_2CO), 4.35 (br s, 0.35H, NCH_2CO), 4.58 (d, 1H, J = 16.2 Hz, NCH*H*Ph), 4.82, 4.89 (s + s, 2H, OCH_2Ph), 7.13 (d, 1H, J = 7.2 Hz, H_{2Bz}, H_{6Bz}), 7.16–7.26 (m, 5H, $H_{6'}$, $H_{7'}$, H_{3Bz}, H_{4Bz}, H_{5Bz}), 7.30–7.35 (m, 2H, $H_{4'}$, $H_{5'}$), 7.35–7.49 (m, 5H, $H_{2''}$, $H_{3''}$, $H_{4''}$, $H_{5''}$, $H_{6''}$), 11.09 (s, 0.15H, CON*H*OCH$_2$Ph), 11.46 (s, 0.75H, CON*H*OCH$_2$Ph); ^{13}C NMR (150.9 MHz, DMSO-d_6) δ (ppm) 30.0 ($C_{3'}$), 33.0 ($C_{2'}$), 38.6 (N*C*H$_2$CO), 43.1 (N*C*H$_2$Ph), 74.9 ($C_{1'}$/C_4), 77.0 (O*C*H$_2$Ph), 123.8 ($C_{7'}$), 125.1 ($C_{4'}$), 127.1 ($C_{6'}$, C_{2Bz}, C_{4Bz}, C_{6Bz}), 128.2 (C_{3Bz}, C_{5Bz}), 128.3 ($C_{2''}$, $C_{4''}$, $C_{6''}$), 128.8 ($C_{3''}$, $C_{5''}$), 129.5 ($C_{5'}$), 135.7 ($C_{1''}$), 137.6 (C_{1Bz}), 138.4 ($C_{7a'}$), 144.7 ($C_{3a'}$), 155.2 (C_2═O), 163.5 (*C*ONHOCH$_2$Ph), 174.5 (C_5═O). Found: C, 71.25; H, 5.60; N, 9.32. Calc. for $C_{27}H_{25}N_3O_4$: C, 71.19; H, 5.53; N, 9.22%.

***N*-Hydroxy-2-(3-benzyl-2,5-dioxo-2′,3′-dihydrospiro-[imidazolidine-4,1′-inden]-1-yl)acetamide (16b).** The *N*-benzyloxy precursor **13b** (250 mg, 0.55 mmol) was subjected to catalytic hydrogenation in a mixture of EtOH/AcOEt 3 : 1 (22 mL) according to the previously described procedure for the synthesis of hydroxamate analogues. Concentration to dryness of the solvents under reduced pressure yielded the title compound **16b** as a white crystalline solid (200 mg, almost quantitative yield); mp melted gradually from 174 °C to 181 °C (from AcOEt/*n*-pentane-dry Et_2O), R_f = 0.49 (AcOEt). In the ^{1}H and ^{13}C NMR spectra of this compound, double set of characteristic peaks are distinguished for each of the two *E*/*Z* conformers. ^{1}H NMR (600.11 MHz, DMSO-d_6) δ (ppm) 2.13 (ddd, 1H, J_1 = 13.9 Hz, J_2 = 8.6 Hz, J_3 = 5.4 Hz, $H_{2'}$), 2.44 (ddd, 1H, J_1 = 13.9 Hz, J_2 = 8.9 Hz, J_3 = 6.1 Hz, $H_{2'}$), 2.92 (ddd, 1H, J_1 = 16.0 Hz, J_2 = 8.5 Hz, J_3 = 6.3 Hz, $H_{3'}$), 2.98 (ddd, 1H, J_1 = 14.4 Hz, J_2 = 8.9 Hz, J_3 = 5.4 Hz, $H_{3'}$), 3.93 (d, 1H, J = 16.3 Hz, NC*H*HPh), 4.04–4.12

(q, AB, 1.5H, J_{AB} = 16.0 Hz, NCH_2CO, *E*-isomer), 4.32–4.40 (q, AB, 0.5H, J_{AB} = 17.4 Hz, NCH_2CO, *Z*-isomer), 4.57 (dd, 1H, J_1 = 16.3 Hz, J_2 = 8.8 Hz, NCH*H*Ph), 7.12 (d, 1H, *J* = 6.7 Hz, H_{2Bz}, H_{6Bz}), 7.15–7.25 (complex m, 5H, $H_{6'}$, $H_{7'}$, H_{3Bz}, H_{4Bz}, H_{5Bz}), 7.29–7.34 (m, 2H, $H_{4'}$, $H_{5'}$), 9.03 (s, 0.68H, CH_2-CONHO*H*, *E*-isomer), 9.41 (s, 0.22H, $NCH_2CONHOH$, *Z*-isomer), 10.37 (s, 0.22H, $NCH_2CONHOH$, *Z*-isomer), 10.80 (s, 0.68H, $CH_2CONHOH$, *E*-isomer); ^{13}C NMR (150.9 MHz, DMSO-d_6) δ (ppm) 30.0 ($C_{3'}$), 32.9, 33.0 ($C_{2'}$), 38.6 (N*C*H_2CO, *E*-isomer), 39.1 (N*C*H_2CO, *Z*-isomer), 43.1 (N*C*H_2Ph), 74.9 ($C_{1'}$/C_4), 123.9 ($C_{7'}$), 125.0 ($C_{4'}$), 127.1 ($C_{6'}$, C_{2Bz}, C_{4Bz}, C_{6Bz}), 128.2 (C_{3Bz}, C_{5Bz}), 129.5 ($C_{5'}$), 137.6 (C_{1Bz}), 138.5 ($C_{7a'}$), 144.7 ($C_{3a'}$), 155.3 (C_2═O, *E*-isomer), 155.5 (C_2═O, *Z*-isomer), 163.2 (NCH_2CO, *E*-isomer), 168.6 (NCH_2CO, *Z*-isomer), 174.6 (C_5═O, *E*-isomer), 174.8 (C_5═O, *Z*-isomer). Found: C, 65.79; H, 5.18; N, 11.55. Calc. for $C_{20}H_{19}N_3O_4$: C, 65.74; H, 5.24; N, 11.50%.

Biology

Cell culture. Huh5-2 (ref. 61) cells (kindly provided by R. Bartenschlager, University of Heidelberg, Germany) contain the subgenomic HCV reporter replicon I_{389}luc-ubi-neo/NS3-3′/Con1/5.1 (genotype 1b; strain Con1). This replicon is composed of the HCV 5′ UTR possessing an internal ribosome entry site (IRES) that directs the expression of a firefly luciferase–ubiquitin–neomycin phosphotransferase fusion protein (luc-ubi-neo). Downstream of this reporter protein is the IRES of the encephalomyocarditis virus (EMCV) that mediates translation of the HCV NS3 to NS5B coding region, followed by the HCV 3′ UTR. The expression of the luc-ubi-neo fusion protein enables the selection for cells containing the replicon using neomycin/G418 and the assessment of viral RNA replication by measuring the activity of the reporter protein firefly luciferase (F-Luc). Stable cell lines Huh7.5-3a and Huh7.5-4a harbor the HCV bicistronic replicons S52-SG (Feo) (AII) and ED43-SG (Feo)(VYG) (kindly provided by C. M. Rice, The Rockefeller University, NY)[67] of the analogous design and were previously described.[68] HCV sequences were derived from the genotype 3a strain S52 and the genotype 4a strain ED43. DENV bicistronic replicon plasmid pD2-hRUPac (kindly provided by C. M. Rice) has been described previously.[69] The structural protein-coding region between capsid gene codon 28 and the last 26 codons at the 3′ end of the envelope gene from an infectious clone of dengue 2 virus (DEN2) 16681 have been replaced by a humanized Renilla luciferase–ubiquitin–puromycin acetyltransferase (hRUPac) cassette. A stable cell line (Huh7-D2) was generated by transfecting Huh7 cells with the above replicon RNA and pooling colonies after selection with 0.5 μg ml^{-1} puromycin. Cells were cultured in high glucose (25 mM) Dulbecco's modified minimal essential medium (Invitrogen), supplemented with 2 mM L-glutamine, 0.1 mM non-essential amino acids, 100 U mL^{-1} penicillin, 100 μg mL^{-1} streptomycin and 10% (v/v) fetal calf serum (referred to as complete DMEM). Complete DMEM was supplemented with 500 μg mL^{-1} G418 for Huh5-2, 750 μg ml^{-1} G418 for Huh7.5-3a, 350 μg mL^{-1} G418 for Huh7.5-4a and 0.5 μg ml^{-1} puromycin for Huh7-D2.

***In vitro* transcription.** Bicistronic DENV constructs were linearized with XbaI and used for *in vitro* transcription as described previously.[70]

Transfection with *in vitro* transcribed RNA. Electroporation with bicistronic DENV RNA into Huh7 cells was performed as described elsewhere.[71]

Cell-based antiviral assays. Replicon assays were performed by seeding 1 × 10^4 cells per well in a 96-well flat bottom plate, cultured in 200 μL complete DMEM supplemented with selection antibiotic. After 24 h incubation at 37 °C (5% CO_2), medium was removed and serial dilutions (without G418) of the test compounds in complete DMEM were added, in a total volume of 100 μL. After 3 days of incubation at 37 °C, cells were lysed and F-Luc or R-Luc activity was measured. Relative luminescence units (RLU) were calculated as percentage of the respective values from DMSO-treated control cells. The half maximal effective concentration (EC_{50}) was defined as the concentration of compound that reduced the luciferase signal by 50%. EC_{50} values were determined by nonlinear regression analysis after converting the drug concentrations into log*X* using the Prism 5.0 software (GraphPad Software Inc.).

Luciferase and Bradford assays. Firefly luciferase (F-Luc) activity in cell lysate was measured using Luciferase Assay System (Promega), as recommended by the manufacturer. Renilla luciferase (R-Luc) activity in cell lysates was measured using 12 μM coelenterazine (Promega) in assay buffer (50 mM potassium phosphate, pH 7.4, 500 mM NaCl, 1 mM EDTA). Measurements were taken in a GloMax 20/20 single-tube luminometer (Promega) for 10 s. Luciferase activities were normalized to the total protein amount determined using the Bradford assay reagent (Bio-Rad).

Cytotoxicity assay. Cytotoxicity of the compounds was determined by measuring intracellular ATP levels. Specifically, 10^4 cells per well were seeded in 96-well flat bottom plates in total volume of 100 μL complete DMEM. After 24 h, cells were incubated with the compounds for 72 h at 37 °C (5% CO_2) and lysed for ATP measurement. Calculation of the compound concentration causing 50% cell death (CC_{50}) was performed using cells treated with DMSO as control sample. CC_{50} values were determined by nonlinear regression analysis after converting the drug concentrations into log*X* using the Prism 5.0 software (GraphPad Software Inc.).

Measurement of intracellular ATP levels. ATP was measured using the ViaLight HS BioAssay kit (Lonza) according to the manufacturer's protocol in a GloMax 20/20 single-tube luminometer (Promega) for 1 s. ATP levels were normalized to total protein amounts.

Indirect immunofluorescence. Indirect immunofluorescence analysis of HCV-4a NS5A was performed as described elsewhere.[71] DNA was stained with propidium iodide (Sigma-Aldrich). Images were acquired with the Leica TCS-SP8 Confocal Microscope.

Total RNA extraction and quantification of viral replicons. Total RNA was extracted from Huh7.5-4a cells using TRIzol

reagent (Ambion), according to the manufacturer's instructions. Replicon RNA was quantified with reverse-transcription (RT) and quantitative real-time polymerase chain reaction (qPCR). For RT, the IRES specific primer 5′-GGATTCGTGCT CATGGTGCA-3′ (reverse) and Moloney murine leukemia virus (MMLV) reverse transcriptase (Promega) were used. For qPCR, the IRES specific primers 5′-GGCCTTGTGGTACTGC CTGATA-3′ (forward) and 5′-GGATTCGTGCTCATGGTGCA-3′ (reverse) and KAPA SYBR FAST qPCR Master Mix (Kapa Biosystems) were used. The housekeeping gene YWHAZ was employed as an internal control (primers 5′-GCTGGTGATGA CAAGAAAGG-3′ and 5′-GGATGTGTTGGTTGCATTTCCT-3′).

Statistical analysis. In all diagrams, bars represent mean values of at least two independent experiments in triplicate. Error bars represent standard deviation. Only results subjected to statistical analysis using Student's *t*-test with $p \leq 0.05$ were considered as statistically significant and presented. Statistical calculations were carried out using Excel Microsoft Office®.

Trypanocidal assays. Bloodstream form *T. brucei* (strain 221) were cultured in modified Iscove's medium, as outlined previously.[72] Eight-point potency curves were performed in 96-well plates (200 μL volumes), and the compound concentrations that inhibited growth by 50% (EC_{50}) and 90% (EC_{90}) were determined. Parasites were first diluted to 2.5×10^4 mL^{-1}, compounds were added at range of concentrations, and the plates incubated at 37 °C. Resazurin was added after 48 h, and the plates incubated for a further 16 h. *T. cruzi* epimastigotes (strain CL Brener) were cultured as previously described.[73] Trypanocidal activity was determined in microtiter plates as outlined above, with the following modifications. Experiments were initiated by seeding the parasites at 2.5×10^5 ml^{-1}, and after the addition of test compounds, cultured at 28 °C for 4 days. Resazurin was added, the plates were incubated for a further 2 days, and then assessed as above. Fluorescence intensities were determined using a BMG FLUOstar Omega (excitation 545 nm, emission 590 nm). Data were analyzed using Graph Pad Prism 7 software. Values are expressed as EC_{50} ± SD and are the average of three independent replicates.

***In vitro* cytotoxicity assays on rat skeletal myoblast L6 cells.** Cytotoxicity against L6 cells was assessed using microtiter plates. Briefly, cells were seeded in triplicate at 1×10^4 mL^{-1} in growth medium containing different compound concentrations. The plates were incubated for 6 days at 37 °C and resazurin then added to each well. After a further 8 h incubation, the fluorescence was determined using a BMG FLUOstar Omega plate reader.

Conflicts of interest

There are no conflicts to declare.

Acknowledgements

E. G. would like to thank the European Federation for Medicinal Chemistry (EFMC) and the editors of the journal for their kind invitation. This work was partially supported by the General Secretariat for Research and Technology (grant KRIPIS II-MIS5002486), by the International Pasteur Network grant ACIP 18-2015 and by the Empirikion Foundation. We would like to thank the State Scholarships Foundation for providing a Ph.D fellowship to E. F. (MIS-5003404) and V. P. (MIS-5000432). We are grateful to Prof. Ralf Bartenschlager (Heidelberg University, Germany) for kindly providing the Huh5-2 cell line and Prof. Charles M. Rice for kindly providing Huh7.5 cells, replicon plasmids S52-SG (Feo) (AII), ED43-SG (Feo) (VYG) and pD2-hRUPac, as well as the 9E10 HCV NS5A-specific antibody.

Notes and references

1 World Health Organization, *Hepatitis C*, http://www.who.int/news-room/fact-sheets/detail/hepatitis-c (accessed March 2019).
2 P. Simmonds, P. Becher, J. Bukh, E. A. Gould, G. Meyers, T. Monath, S. Muerhoff, A. Pletnev, R. Rico-Hesse, D. B. Smith and J. T. Stapleton, *J. Gen. Virol.*, 2017, **98**, 2–3.
3 R. Bartenschlager, V. Lohmann and F. Penin, *Nat. Rev. Microbiol.*, 2013, **11**, 482–496.
4 D. Moradpour, F. Penin and C. M. Rice, *Nat. Rev. Microbiol.*, 2007, **5**, 453–463.
5 S. Ramirez and J. Bukh, *Antiviral Res.*, 2018, **158**, 264–287.
6 J. P. Messina, I. Humphreys, A. Flaxman, A. Brown, G. S. Cooke, O. G. Pybus and E. Barnes, *Hepatology*, 2015, **61**, 77–87.
7 V. Soriano, M. G. Peters and S. Zeuzem, *Clin. Infect. Dis.*, 2009, **48**, 313–320.
8 *VOSEVI (sofosbuvir, velpatasvir, and voxilaprevir) tablets: FDA Highlights of Prescibing Information*, https://www.accessdata.fda.gov/drugsatfda_docs/label/2017/209195s000lbl.pdf, (accessed 7 May 2019).
9 *DAKLINZA (daclatasvir) tablets: FDA Highlights of Prescribing Information*, https://www.accessdata.fda.gov/drugsatfda_docs/label/2017/206843s006lbl.pdf, (accessed 7 May 2019).
10 *SOVALDI (sofosbuvir) tablets: FDA Highlights of Prescribing Information*, https://www.accessdata.fda.gov/drugsatfda_docs/label/2015/204671s002lbl.pdf, (accessed 7 May 2019).
11 *VIEKIRA PAK (ombitasvir, paritaprevir and ritonavir tablets; dasabuvir tablets): FDA Highlights of Prescibing Information*, https://www.accessdata.fda.gov/drugsatfda_docs/label/2014/206619lbl.pdf, (accessed 7 May 2019).
12 *The American Association for the Study of Liver Disease*, http://www.hcvguidelines.org (accessed March 2019).
13 J. M. Pawlotsky, F. Negro, A. Aghemo, M. Berenguer, O. Dalgard, G. Dusheiko, F. Marra, M. Puoti and H. Wedemeyer, *J. Hepatol.*, 2018, **69**, 461–511.
14 T. Asselah, P. Marcellin and R. F. Schinazi, *Liver Int.*, 2018, **38**(Suppl 1), 7–13.
15 V. Gimeno-Ballester, M. Buti, R. San Miguel, M. Riveiro and R. Esteban, *J. Viral Hepatitis*, 2017, **24**, 904–916.
16 C. Hézode, P. Lebray, V. De Ledinghen, F. Zoulim, V. Di Martino, N. Boyer, D. Larrey, D. Botta-Fridlund, C. Silvain,

H. Fontaine, L. D'Alteroche, V. Leroy, M. Bourliere, I. Hubert-Fouchard, D. Guyader, I. Rosa, E. Nguyen-Khac, L. Fedchuk, R. Akremi, Y. Bennai, A. Filipovics, Y. Zhao and J. P. Bronowicki, *Liver Int.*, 2017, **37**, 1314–1324.

17 L. Cuypers, F. Ceccherini-Silberstein, K. Van Laethem, G. Li, A. M. Vandamme and J. K. Rockstroh, *Rev. Med. Virol.*, 2016, **26**, 408–434.

18 H. Barth, *World J. Hepatol.*, 2015, **7**, 725–737.

19 J. D. Stanaway, D. S. Shepard, E. A. Undurraga, Y. A. Halasa, L. E. Coffeng, O. J. Brady, S. I. Hay, N. Bedi, I. M. Bensenor, C. A. Castañeda-Orjuela, T. W. Chuang, K. B. Gibney, Z. A. Memish, A. Rafay, K. N. Ukwaja, N. Yonemoto and C. J. L. Murray, *Lancet Infect. Dis.*, 2016, **16**, 712–723.

20 A. S. Leong, K. T. Wong, T. Y. Leong, P. H. Tan and P. Wannakrairot, *Semin. Diagn. Pathol.*, 2007, **24**, 227–236.

21 S. R. Hadinegoro, J. L. Arredondo-Garcia, M. R. Capeding, C. Deseda, T. Chotpitayasunondh, R. Dietze, H. I. Muhammad Ismail, H. Reynales, K. Limkittikul, D. M. Rivera-Medina, H. N. Tran, A. Bouckenooghe, D. Chansinghakul, M. Cortes, K. Fanouillere, R. Forrat, C. Frago, S. Gailhardou, N. Jackson, F. Noriega, E. Plennevaux, T. A. Wartel, B. Zambrano, M. Saville and CYD-TDV Dengue Vaccine Working Group, *N. Engl. J. Med.*, 2015, **373**, 1195–1206.

22 J. G. Low, E. E. Ooi and S. G. Vasudevan, *J. Infect. Dis.*, 2017, **215**, S96–S102.

23 R. Bartenschlager and S. Miller, *Future Microbiol.*, 2008, **3**, 155–165.

24 M. S. Diamond and T. C. Pierson, *Cell*, 2015, **162**, 488–492.

25 M. Stempniak, Z. Hostomska, B. R. Nodes and Z. Hostomsky, *J. Virol.*, 1997, **71**, 2881–2886.

26 D. N. Frick, S. Banik and R. S. Rypma, *J. Mol. Biol.*, 2007, **365**, 1017–1032.

27 P. J. Lim, U. Chatterji, D. Cordek, S. D. Sharma, J. A. Garcia-Rivera, C. E. Cameron, K. Lin, P. Targett-Adams and P. A. Gallay, *J. Biol. Chem.*, 2012, **287**, 30861–30873.

28 S. Bressanelli, L. Tomei, F. A. Rey and R. De Francesco, *J. Virol.*, 2002, **76**, 3482–3492.

29 R. B. Davidson, J. Hendrix, B. J. Geiss and M. McCullagh, *PLoS Comput. Biol.*, 2018, **14**, e1006103.

30 T. L. Yap, T. Xu, Y. L. Chen, H. Malet, M. P. Egloff, B. Canard, S. G. Vasudevan and J. Lescar, *J. Virol.*, 2007, **81**, 4753–4765.

31 World Health Organization, *Trypanosomiasis, human African (sleeping sickness)*, https://www.who.int/news-room/fact-sheets/detail/trypanosomiasis-human-african-(sleeping-sickness) (accessed March 2019).

32 E. Bottieau and J. Clerinx, *Infect. Dis. Clin. North Am.*, 2019, **33**, 61–77.

33 S. Varikuti, B. K. Jha, G. Volpedo, N. M. Ryan, G. Halsey, O. M. Hamza, B. S. McGwire and A. R. Satoskar, *Front. Microbiol.*, 2018, **9**, 2655.

34 P. G. E. Kennedy and J. Rodgers, *Front. Immunol.*, 2019, **10**, 39.

35 C. H. Baker and S. C. Welburn, *Trends Parasitol.*, 2018, **34**, 818–827.

36 R. J. Wall, E. Rico, I. Lukac, F. Zuccotto, S. Elg, I. H. Gilbert, Y. Freund, M. R. K. Alley, M. C. Field, S. Wyllie and D. Horn, *Proc. Natl. Acad. Sci. U. S. A.*, 2018, **115**, 9616–9621.

37 F. Chappuis, *Lancet*, 2018, **391**, 100–102.

38 World Health Organization, *Chagas disease (American trypanosomiasis)* https://www.who.int/news-room/fact-sheets/detail/chagas-disease-(american-trypanosomiasis (accessed March 2019).

39 A. Rassi, J. M. de Rezende, A. O. Luquetti and A. Rassi Jr, in *American Trypanosomiasis Chagas Disease: One Hundred Years of Research*, ed. J. Telleria and M. Tibayrenc, Elsevier, Amsterdam (Netherlands), 2nd edn, 2017, vol. 28, pp. 653–686.

40 J. Bermudez, C. Davies, A. Simonazzi, J. P. Real and S. Palma, *Acta Trop.*, 2016, **156**, 1–16.

41 Q. P. Wang, T. Kawahara and D. Horn, *Mol. Microbiol.*, 2010, **77**, 1237–1245.

42 M. D. Urbaniak, A. Crossman, T. Chang, T. K. Smith, D. M. F. van Aalten and M. A. J. Ferguson, *J. Biol. Chem.*, 2005, **280**, 22831–22838.

43 G. F. Mercaldi, H. M. Pereira, A. T. Cordeiro, P. A. M. Michels and O. H. Thiemann, *FEBS J.*, 2012, **279**, 2012–2021.

44 C. Gong, A. Martins and S. Shuman, *J. Biol. Chem.*, 2003, **278**, 50843–50852.

45 S. R. Wilkinson, S. R. Prathalingam, M. C. Taylor, A. Ahmed, D. Horn and J. M. Kelly, *Free Radical Biol. Med.*, 2006, **40**, 198–209.

46 S. K. Menzies, L. B. Tulloch, G. J. Florence and T. K. Smith, *Parasitology*, 2016, **145**, 175–183.

47 S. Wyllie and A. H. Fairlamb, *Semin. Cell Dev. Biol.*, 2011, **22**, 271–277.

48 D. R. de Menezes, C. M. Calvet, G. C. Rodrigues, M. C. de Souza Pereira, I. R. Almeida, A. P. de Aguiar, C. T. Supuran and A. B. Vermelho, *J. Enzyme Inhib. Med. Chem.*, 2016, **31**, 964–973.

49 A. A. Zuma and W. D. Souza, *Future Sci. OA*, 2018, **4**, FSO325.

50 M. D. Urbaniak, A. S. Capes, A. Crossman, S. O'Neill, S. Thompson, I. H. Gilbert and M. A. J. Ferguson, *Carbohydr. Res.*, 2014, **387**, 54–58.

51 G. U. Ebiloma, E. O. Balogun, E. J. Cueto-Díaz, H. P. de Koning and C. Dardonville, *Med. Res. Rev.*, 2019, DOI: 10.1002/med.21560.

52 P. Smith, C. K. Ho, Y. Takagi, H. Djaballah and S. Shuman, *mBio*, 2016, **7**, e00058.

53 E. Giannakopoulou, V. Pardali and G. Zoidis, *Future Med. Chem.*, 2018, **10**, 1283–1285.

54 A. Y. Chen, R. N. Adamek, B. L. Dick, C. V. Credille, C. N. Morrison and S. M. Cohen, *Chem. Rev.*, 2018, **119**, 1323–1455.

55 L. Riccardi, V. Genna and M. De Vivo, *Nat. Rev. Chem.*, 2018, **2**, 100–112.

56 G. Zoidis, E. Giannakopoulou, A. Stevaert, E. Frakolaki, V. Myrianthopoulos, G. Fytas, P. Mavromara, E. Mikros, R. Bartenschlager, N. Vassilaki and L. Naesens, *Med. Chem. Commun.*, 2016, **7**, 447–456.

57 C. Fytas, G. Zoidis, N. Tzoutzas, M. C. Taylor, G. Fytas and J. M. Kelly, *J. Med. Chem.*, 2011, **54**, 5250–5254.
58 G. Zoidis, A. Tsotinis, A. Tsatsaroni, M. C. Taylor, J. M. Kelly, A. Efstathiou, D. Smirlis and G. Fytas, *Chem. Biol. Drug Des.*, 2018, **91**, 408–421.
59 E. Giannakopoulou, V. Pardali, I. Skrettas and G. Zoidis, *ChemistrySelect*, 2019, **4**, 3195–3198.
60 C. Fytas, G. Zoidis and G. Fytas, *Tetrahedron*, 2008, **64**, 6749–6754.
61 J. M. Vrolijk, A. Kaul, B. E. Hansen, V. Lohmann, B. L. Haagmans, S. W. Schalm and R. Bartenschlager, *J. Virol. Methods*, 2003, **110**, 201–209.
62 Marvin was used for determining logD, *Marvin 5.12.2*, 2013, ChemAxon (http://www.chemaxon.com).
63 *Schrödinger Release 2019–1: Jaguar pKa*, Schrödinger, LLC, New York, NY, 2019.
64 A. D. Bochevarov, M. A. Watson, J. R. Greenwood and D. M. Philipp, *J. Chem. Theory Comput.*, 2016, **12**, 6001–6019.
65 H. S. Yu, M. A. Watson and A. D. Bochevarov, *J. Chem. Inf. Model.*, 2018, **58**, 271–286.
66 J. J. Klicić, R. A. Friesner, S. Y. Liu and W. C. Guida, *J. Phys. Chem. A*, 2002, **106**, 1327–1335.
67 M. Saeed, T. K. Scheel, J. M. Gottwein, S. Marukian, L. B. Dustin, J. Bukh and C. M. Rice, *Antimicrob. Agents Chemother.*, 2012, **56**, 5365–5373.
68 N. Lougiakis, E. Frakolaki, P. Karmou, N. Pouli, P. Marakos, V. Madan, R. Bartenschlager and N. Vassilaki, *Chem. Biol. Drug Des.*, 2017, **90**, 352–367.
69 J. Dufner-Beattie, A. O'Guin, S. O'Guin, A. Briley, B. Wang, J. Balsarotti, R. Roth, G. Starkey, U. Slomczynska, A. Noueiry, P. D. Olivo and C. M. Rice, *Antimicrob. Agents Chemother.*, 2014, **58**, 3399–3410.
70 A. Kaul, I. Woerz, P. Meuleman, G. Leroux-Roels and R. Bartenschlager, *J. Virol.*, 2007, **81**, 13168–13179.
71 N. Vassilaki, P. Friebe, P. Meuleman, S. Kallis, A. Kaul, G. Paranhos-Baccalà, G. Leroux-Roels, P. Mavromara and R. Bartenschlager, *J. Virol.*, 2008, **82**, 11503–11515.
72 M. C. Taylor, A. P. McLatchie and J. M. Kelly, *Mol. Microbiol.*, 2013, **89**, 420–432.
73 G. Kendall, A. F. Wilderspin, F. Ashall, M. A. Miles and J. M. Kelly, *EMBO J.*, 1990, **9**, 2751–2758.

